Metal-Insulator Transitions in a model for magnetic Weyl semimetal and graphite under high magnetic field

- Disorder-driven quantum phase transition in Weyl fermion semimetal

Luo, Xu, Ohtsuki and RS, ArXiv:1710.00572v2,

Liu, Ohtsuki and RS, Phys. Rev. Lett. 116, 066401 (2016)

Xunlong Luo (PKU), Shang Liu (PKU -> Harvard),
Baolong Xu (PKU), Tomi Ohtsuki (Sophia Univ.)

- Correlation-driven metal-insulator transition in graphite under H

Zhang and RS, Phys. Rev. B 95, 205108 (2017)

Pan and RS, in preparation

Zhiming Pan (PKU), Xiaotian Zhang (PKU), Ryuichi Shindou (PKU)

Content

- **Disorder-driven quantum phase transition in Weyl fermion semimetal**
  - Quantum multicriticality with spatially anisotropic scaling
  - DOS, conductivity, and diffusion constant scalings near Weyl nodes
  - Unconventional critical exponent associated with 3D band insulator-Weyl semimetal transition
- **Correlation-driven metal-insulator transition in graphite under H**
  - experiments, previous theories and issues to be addressed
  - charge neutrality point, Umklapp term, RG argument
  - Mott insulator with spin nematic orders, phenomenology of graphite under high H

- Weyl fermion semimetal (WSM) and magnetic WSM

  - Discovery of Weyl fermion semimetal in TaAs, TaP, … (non-magnetic WSM)

  - Nielsen-Ninomiya Theorem

    Nielsen-Ninomiya (1981)

    Two Weyl fermions with opposite magnetic charge appear in pair in the k-space

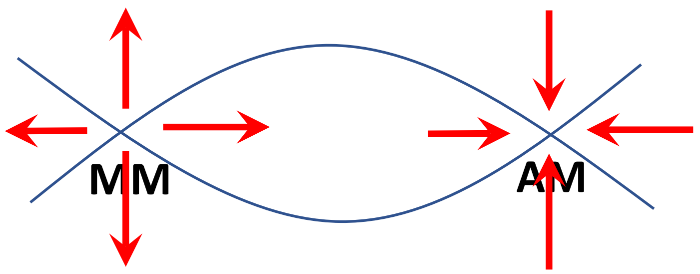

Magnetic WSM (mWSM)

  - Novel magneto-transport properties, related to chiral anomaly in 3+1 D

    Burkov-Balents (2011), Vazifeh-Franz (2013), . . .

  - Disorder-driven semimetal-metal quantum phase transition

    Fradkin (1986), . . .

□ Disorder-driven semimetal-metal quantum phase transition in mWSM

Fradkin (1986), . . .

renormalized WSM **Diffusive Metal (DM)**

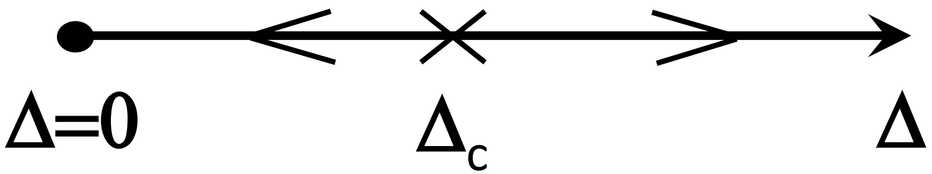

renormalized WSM : zero-energy DOS = 0

DM : zero-energy DOS evolves continuously from zero

■ DOS scaling and zero-energy conductivity near Weyl node

Kobayashi et.al. (2014), . . .

Kobayashi et.al. (2014)

Non-magnetic WSM

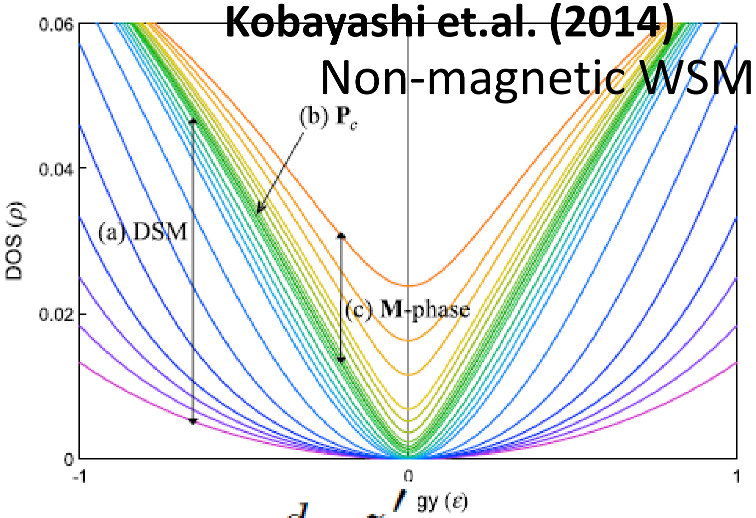

Liu et.al. (2016)

Magnetic WSM

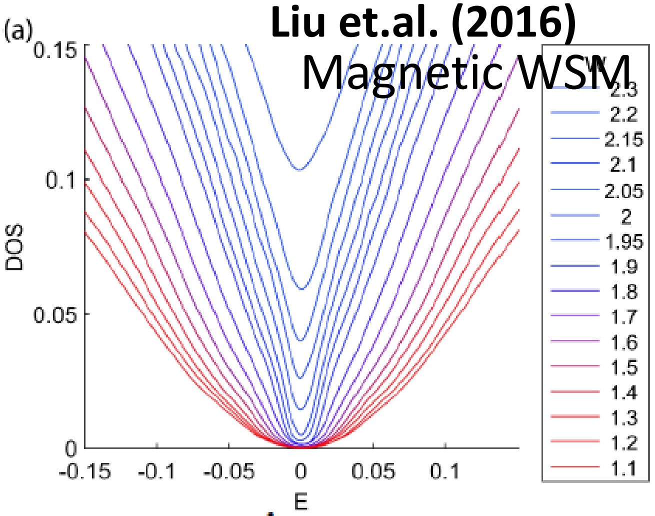

Wegner's relation

$$|\delta\overline{\Delta}_0|^{\frac{d-2}{y'_\Delta}}$$

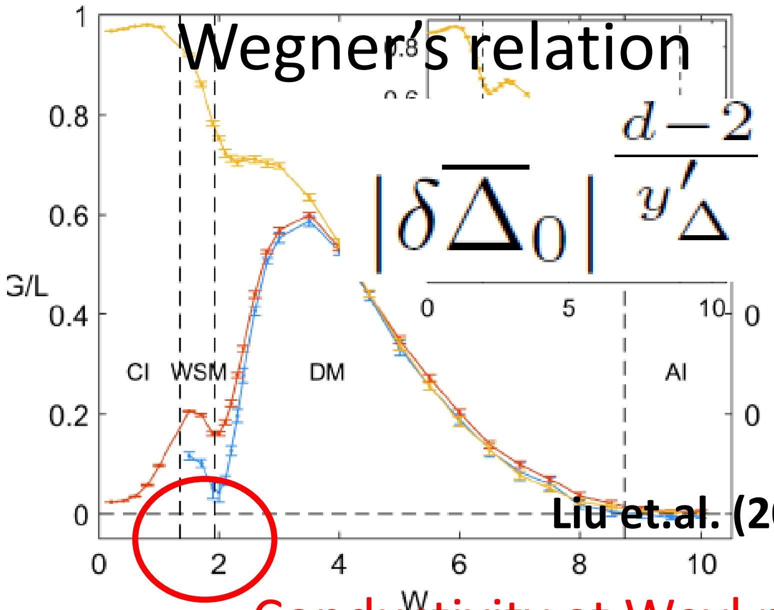

Liu et.al. (2016)

Conductivity at Weyl node vanishes at QCP

$$\delta\overline{\Delta}_0^{\frac{d-z'}{y'_\Delta}} \quad \text{(DM)}$$

$$|\delta\overline{\Delta}_0|^{-\frac{dz'-d}{y'_\Delta}}|\mathcal{E}|^{d-1} \quad \text{(WSM)}$$

☐ Disorder-driven Quantum Multicritlcality in disordered WSM (this work)

Luo, Xu, Ohtsuki and RS, ArXiv:1710.00572v2

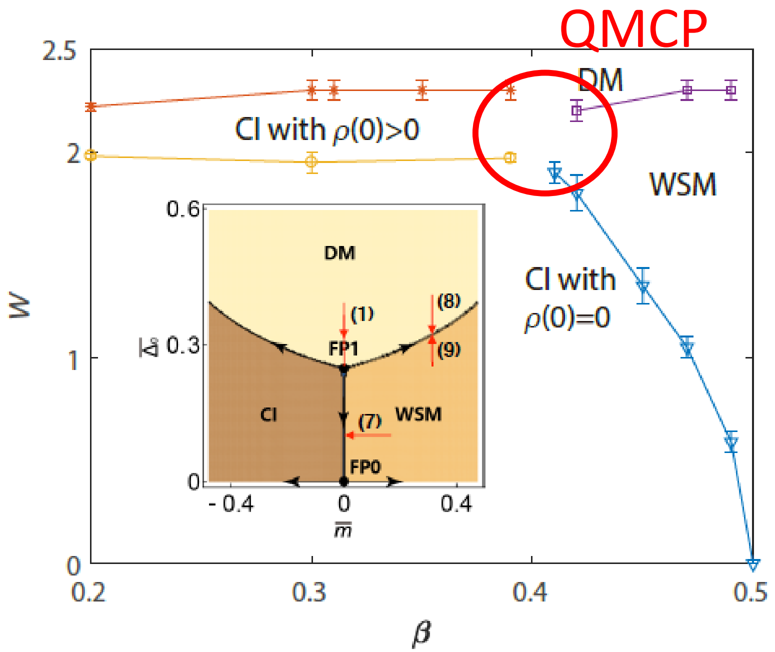

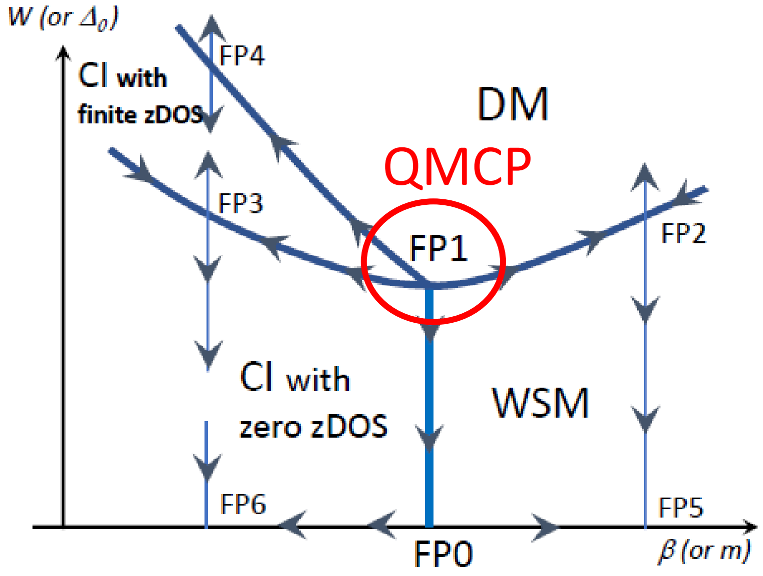

- Quantum Multicritical Point with two parameter scalings
- Spatially anisotropic scaling for conductivity and Diffusion Constant near Weyl node around QMCP and quantum phase transition line between CI and WSM

  - Conductivity and diffusion constant along one spatial direction obey different universal function with different exponents from that along the other spatial direction.
  - `Magnetic dipole' model at FP0 (fixed point in the clean limit)

    The anisotropy comes from a magnetic dipole in the k-space

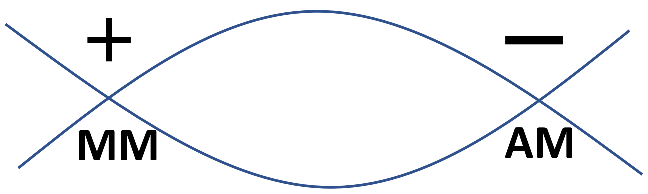

☐ Disorder-driven Quantum Multicritlcality in disordered WSM (this work)

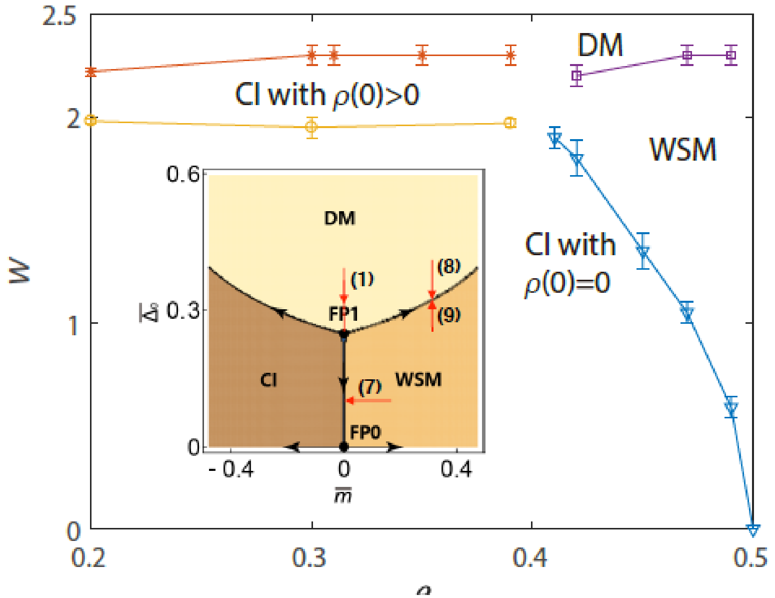

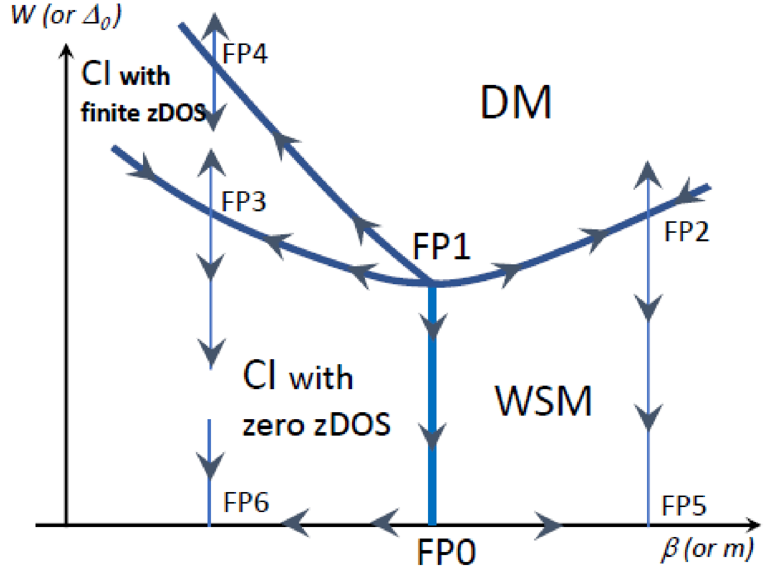

■ For CI-DM branch, a mobility edge and band edge are distinct from each other in the phase diagram (For DM-WSM branch, where they are identical).

DOS at nodes has scaling property

conductivity at nodes has scaling property (conventional 3D unitary class)

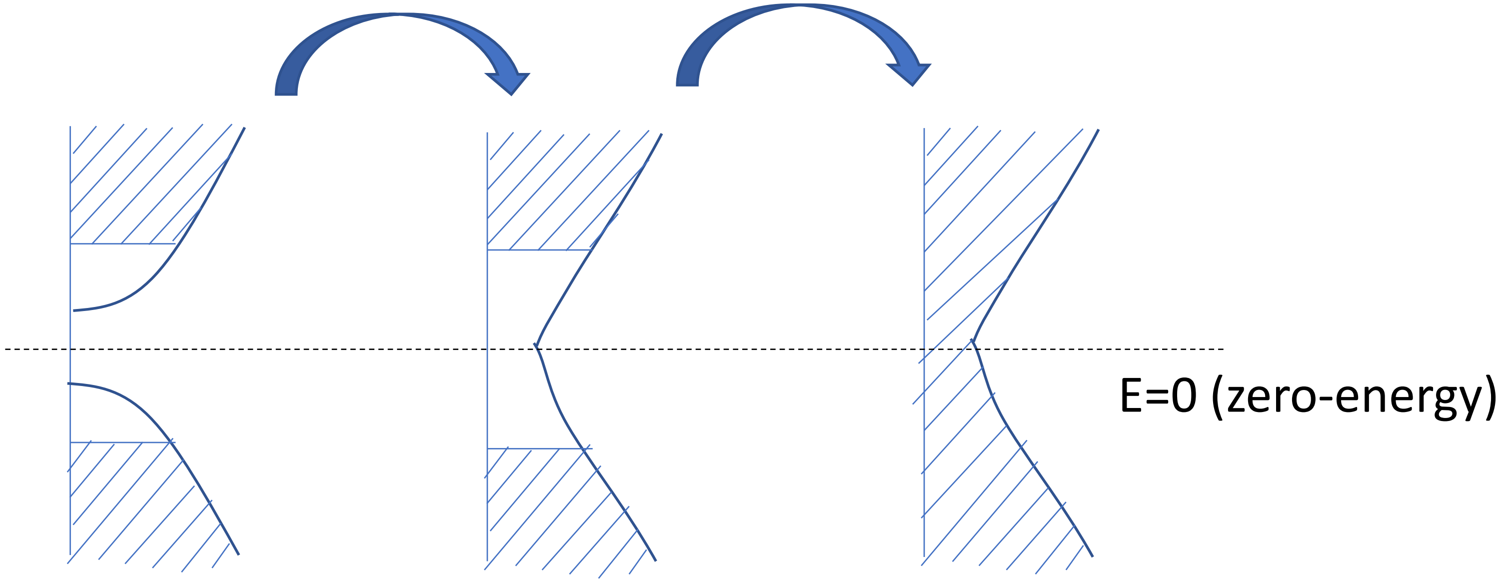

CI phase with zero zero-energy DOS

CI phase with finite zero-energy DOS

Diffusive metal (DM) phase

☐ Disorder-driven Quantum Multicritlcality in disordered WSM (this work)

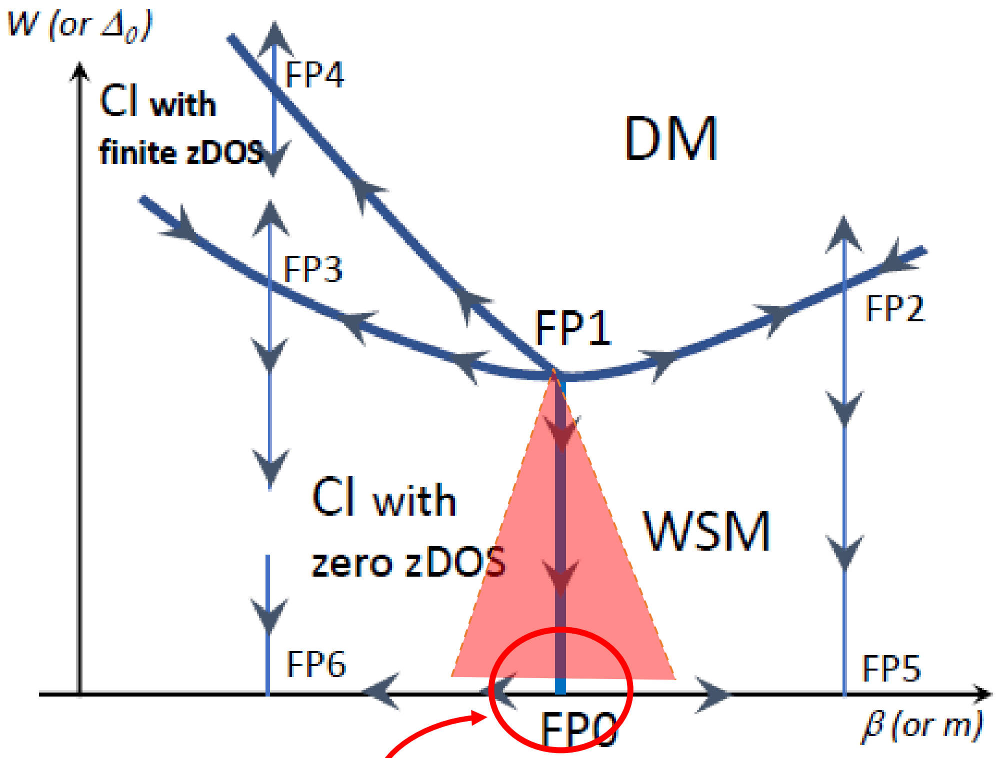

$$\xi_3 = m^{-\frac{1}{2}},\ \xi_\perp = m^{-1}$$

ν = 0.5 ν=1.0

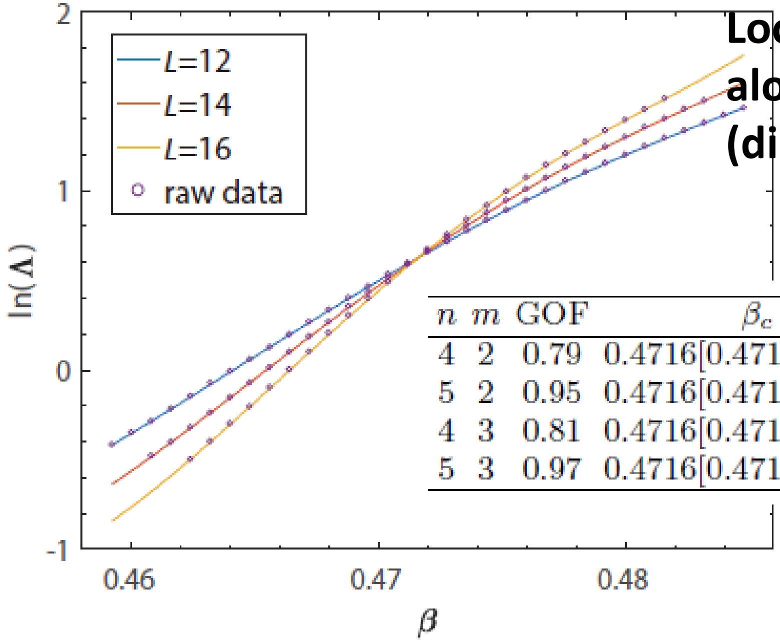

Localization length along 3-direction (dipole direction)

n	m	GOF	β_c	ν
4	2	0.79	0.4716[0.4715,0.4716]	0.8008[0.7947,0.8068]
5	2	0.95	0.4716[0.4715,0.4716]	0.8002[0.7943,0.8069]
4	3	0.81	0.4716[0.4715,0.4717]	0.8097[0.7964,0.8225]
5	3	0.97	0.4716[0.4715,0.4716]	0.8124[0.7990,0.8261]

- For CI-WSM branch, a transition is direct, whose critical exponent is evaluated as 0.80 ±0.01 !?
  - Disorder average out the spatial anistorpy; 1/3 (0.5+1+1) = 0.8333?
  - Crossover behavior from FP1 and FP0 ? large-n RG analysis ➔ ν = 1/(2–2/n) = 1 @ FP1

In other words, data points could range from the critical regime to its outside.

◻ Magnetic dipole model

Roy, et.al. (2016), Luo, et.al. (2017)

$$\mathcal{H}_{\rm eff} = \int d^2\boldsymbol{x}_\perp dx_3\, \psi^\dagger(\boldsymbol{x})\Big\{ -iv(\partial_1\boldsymbol{\sigma}_1 + \partial_2\boldsymbol{\sigma}_2) + \big((-i)^2 b_2\partial_3^2 - m\big)\boldsymbol{\sigma}_3 \Big\}\psi(\boldsymbol{x}),$$

where $\boldsymbol{x}_\perp \equiv (x_1, x_2)$

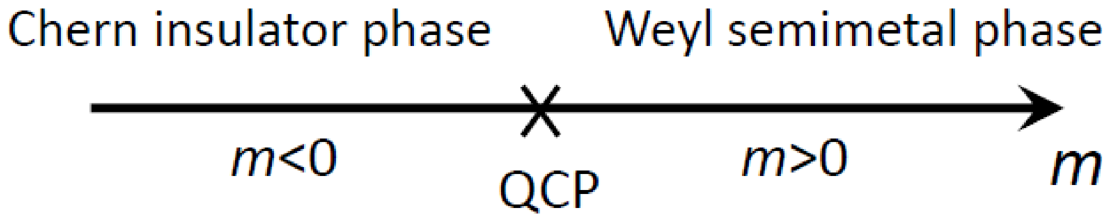

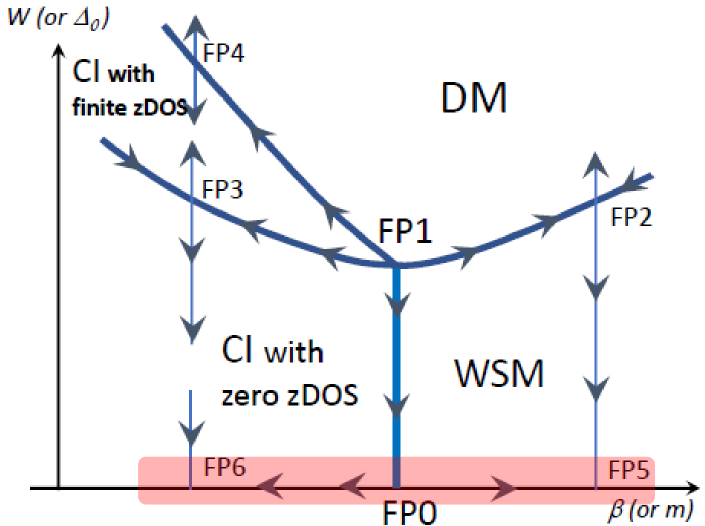

m>0 : WSM phase

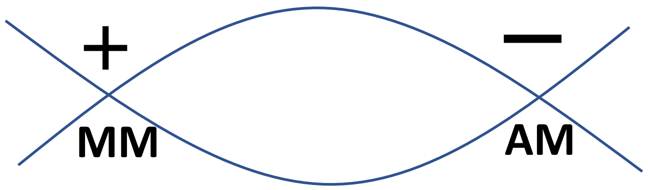

MM and AM locate at $(p_1, p_2, p_3) = (0, 0, \pm\sqrt{m/b_2})$.

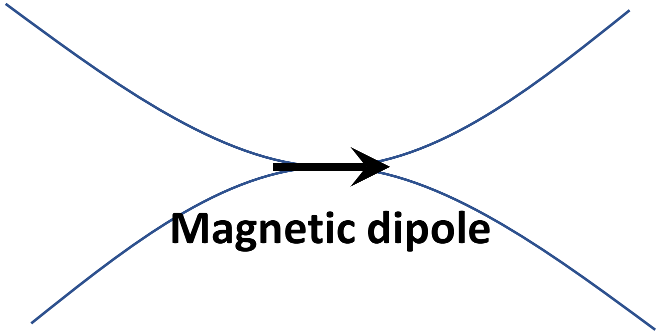

m=0 : a critical point Between WSM phase and 3D Chern band insulator

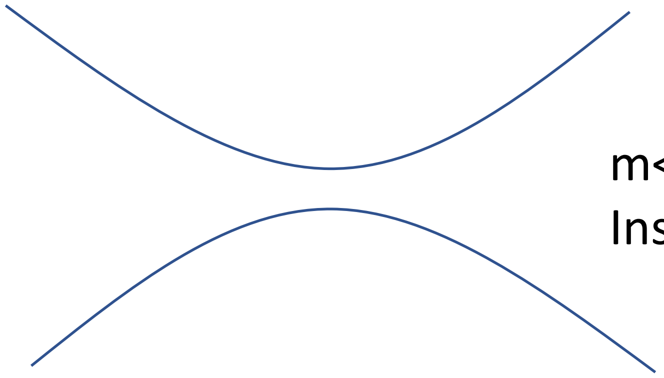

m<0 : 3D Chern band Insulator (CI) phase

Effect of Disorders on Magnetic dipole model

A tree-level argument on replicated effective action

$$Z = \int d\psi^{\dagger}_{\alpha}\psi_{\alpha} e^{-S}, \quad S = S_0 + S_1,$$

$$S_0 \equiv \int d\tau \int d^2\boldsymbol{x}_{\perp} dx_3\, \psi^{\dagger}_{\alpha}(\boldsymbol{x},\tau)\Big\{a\partial_{\tau} - iv(\partial_1\boldsymbol{\sigma}_1 + \partial_2\boldsymbol{\sigma}_2) + ((-i)^2 b_2\partial_3^2 - m)\boldsymbol{\sigma}_3\Big\}\psi_{\alpha}(\boldsymbol{x},\tau)$$

$$S_1 \equiv -\frac{\Delta_0}{2}\int d\tau \int d\tau' \int d^3\boldsymbol{x}\, (\psi^{\dagger}_{\alpha}\psi_{\alpha})_{\boldsymbol{x},\tau}(\psi^{\dagger}_{\beta}\psi_{\beta})_{\boldsymbol{x},\tau'} - \cdots$$

Free part :

$$\underbrace{b^{-(d-\frac{1}{2})}}_{\psi^{\dagger}\psi} \cdot \underbrace{b^{-1} \cdot b^{d-1+\frac{1}{2}+1}}_{\partial_1 d^{d-1}\boldsymbol{x}_{\perp} dx_3 d\tau} = b^0$$

Disorder (\`interaction') part :

$$\underbrace{b^{-2(d-\frac{1}{2})}}_{\psi^{\dagger}\psi^{\dagger}\psi\psi} \cdot \underbrace{b^{d-1+\frac{1}{2}+2}}_{d^{d-1}\boldsymbol{x}_{\perp} dx_3 d\tau d\tau'} = b^{-(d-\frac{5}{2})}$$

To make S_0 at the massless point (m=0) to be scale-invariant, . . .

$$\boxed{\begin{aligned} x_3' &= b^{\frac{1}{2}} x_3, \\ \boldsymbol{x}_{\perp}' &= b\boldsymbol{x}_{\perp}, \\ \tau' &= b\tau \\ \psi' &= b^{-\frac{1}{2}(d-\frac{1}{2})}\psi \\ m' &= b^{-1} m \end{aligned}}$$

with $b \equiv e^{-dl} < 1$

with prime : After RG
Without prime : Before RG

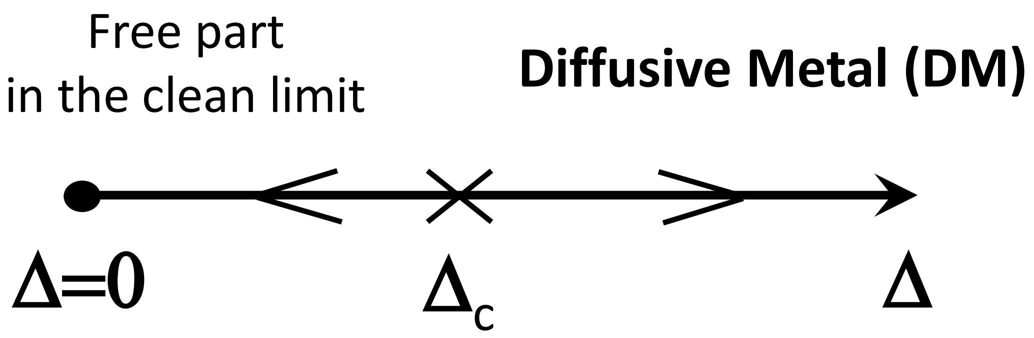

Effect of Disorders on Magnetic dipole model

- One-loop level RG (large-n expansion analysis ; n=2)

$$\frac{dm}{dl} = m(1-2\overline{\Delta}_0),$$
$$\frac{d\overline{\Delta}_0}{dl} = -\frac{1}{2}\overline{\Delta}_0 + 2\overline{\Delta}_0^2,$$
$$z = 1 + 2\overline{\Delta}_0,$$

where $\overline{\Delta}_0 \equiv \Delta_0 \frac{(v\Lambda)^{\frac{1}{2}}}{4\pi^2 v^2 b_2^{\frac{1}{2}}}$

Roy, et.al. (2016), Luo, et.al. (2017)

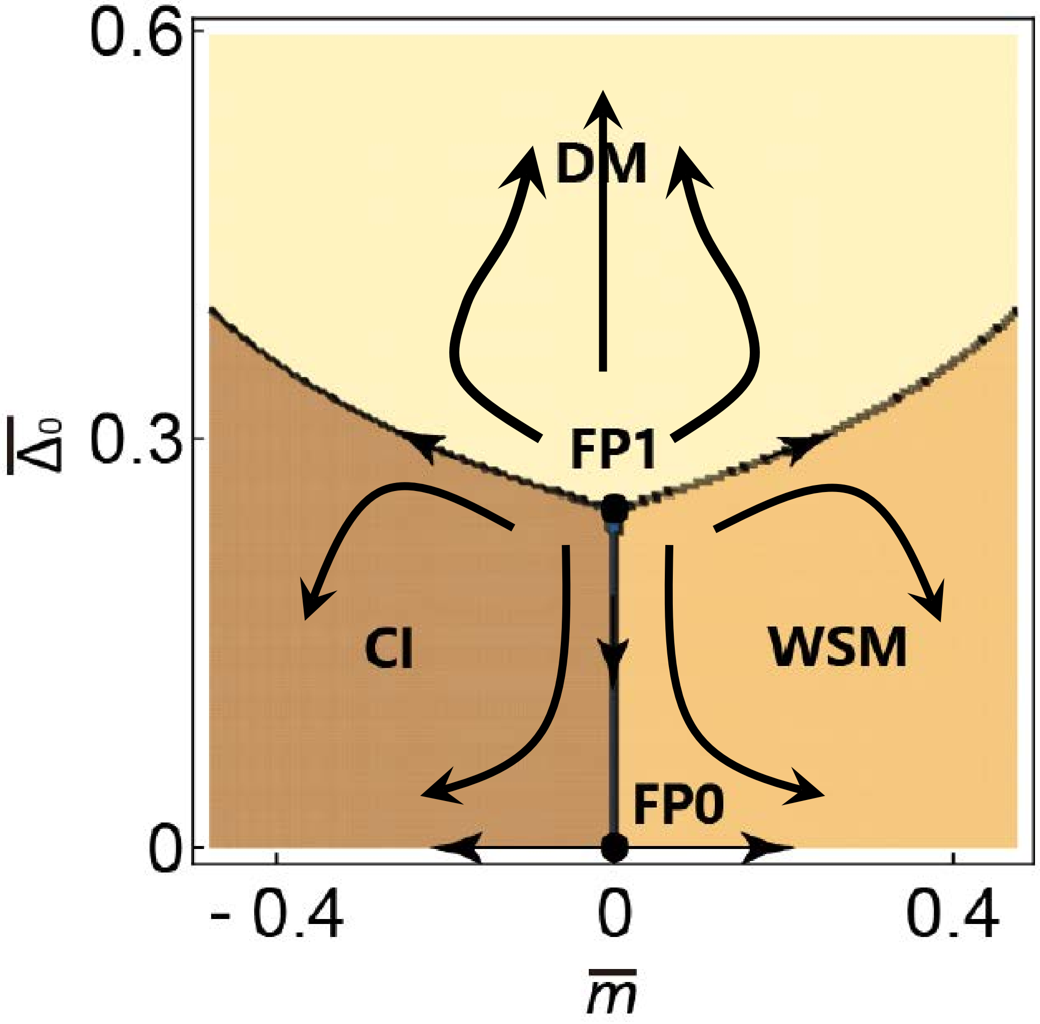

Effect of Disorders on Magnetic dipole model

- One-loop level RG (large-n expansion analysis ; n=2)

Roy, et.al. (2016), Luo, et.al. (2017)

$$\frac{dm}{dl} = m(1 - 2\overline{\Delta}_0),$$
$$\frac{d\overline{\Delta}_0}{dl} = -\frac{1}{2}\overline{\Delta}_0 + 2\overline{\Delta}_0^2,$$
$$z = 1 + 2\overline{\Delta}_0,$$

FP0: a saddle-point fixed point with one relevant scaling variable and one irrelevant variable

$$(z, \overline{\Delta}_0) = (1, 0)$$
$$[\overline{\Delta}_0] \equiv y_{\overline{\Delta}_0} = -(d - \frac{5}{2}) = -\frac{1}{2}$$
$$[m] \equiv y_{\overline{m}} = 1$$

FP1: an unstable fixed point with relevant scaling variables

$$(z, \overline{\Delta}_0) = (1 + \frac{1}{n}, \frac{1}{2n}) = (\frac{3}{2}, \frac{1}{4})$$
$$[\delta\overline{\Delta}_0] \equiv y_\Delta = \frac{1}{n} = \frac{1}{2}$$
$$[m] \equiv y_m = 1 - \frac{1}{n} = \frac{1}{2}$$

where $\delta\overline{\Delta}_0 \equiv \overline{\Delta}_0 - \Delta_c$

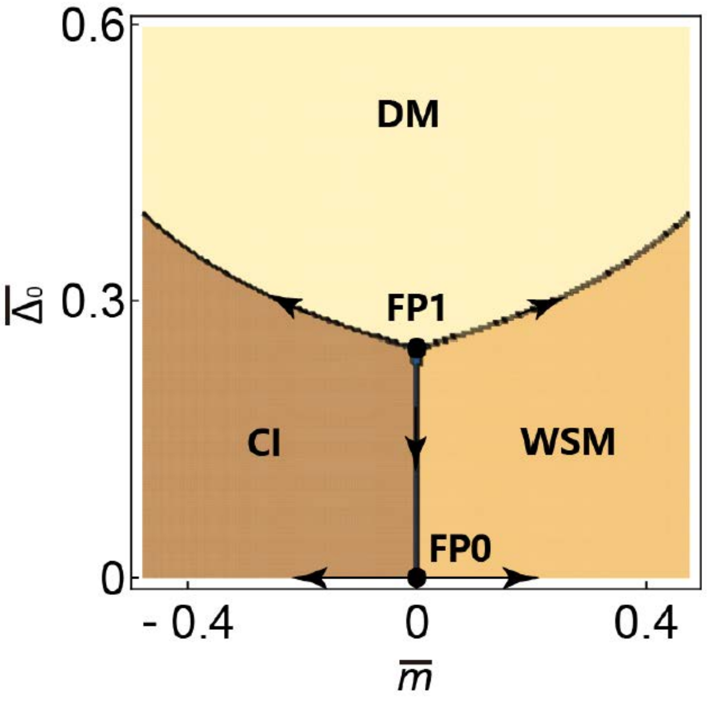

Effect of Disorders on Magnetic dipole model

- For positively larger m, ...

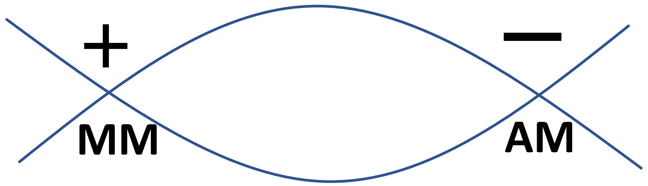

MM and AM locate at $(p_1, p_2, p_3) = (0, 0, \pm\sqrt{m/b_2})$.

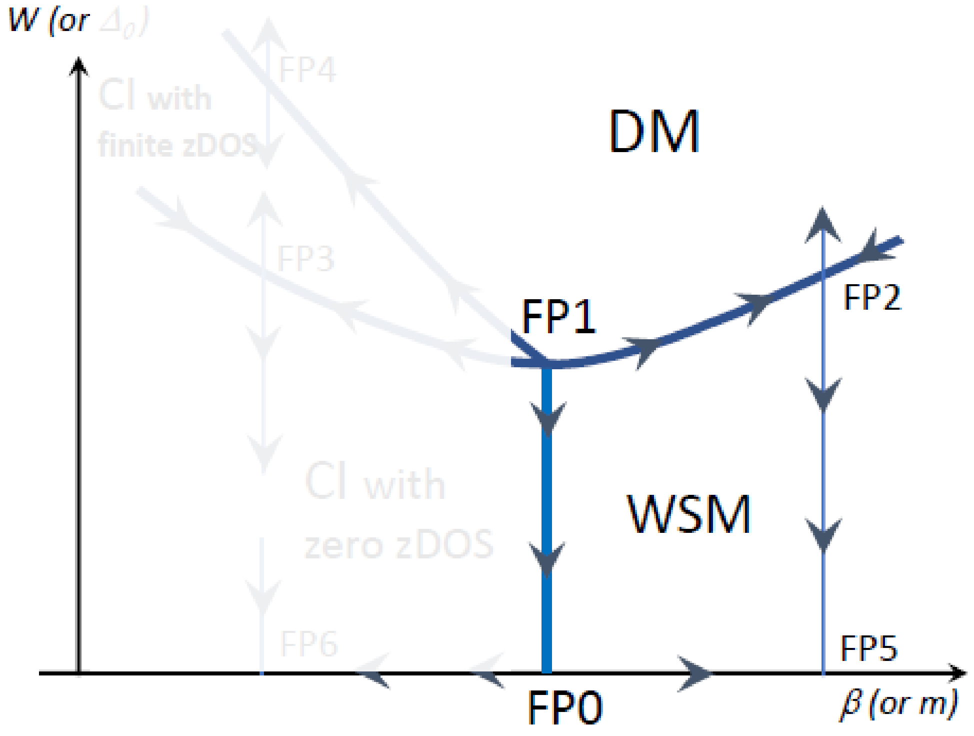

Low energy effective Hamiltonian (E<m)

: disordered single-Weyl node

$$\mathcal{H}_{\text{eff}} = \int d^2\boldsymbol{x}_\perp dx_3\, \psi^\dagger(\boldsymbol{x})\Big\{ -iv(\partial_1\boldsymbol{\sigma}_1 + \partial_2\boldsymbol{\sigma}_2 \pm iv_3\boldsymbol{\sigma}_3\Big\}\psi(\boldsymbol{x}),$$

Fradkin (1986), ...

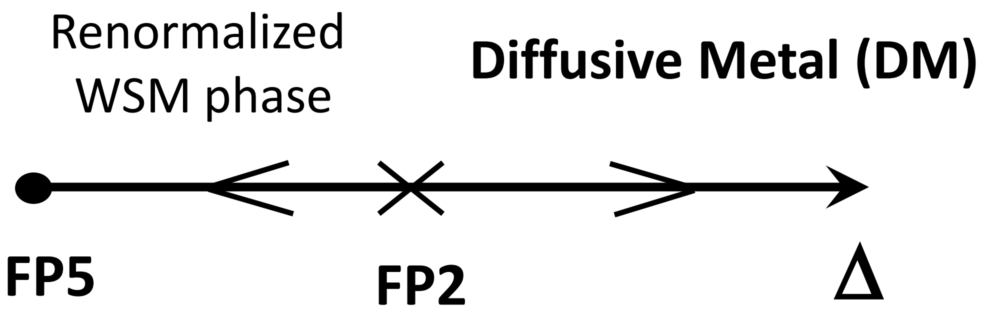

Scaling Theories of DOS, Diffusion Constant and conductivities

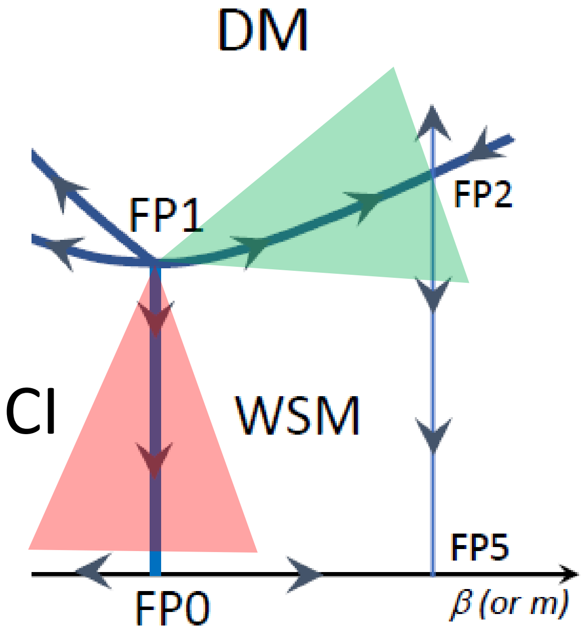

- Critical Property near CI-WSM boundary is controlled by FP0
- Critical Property near WSM-DM boundary is controlled by FP2
- The system has gapless electronic dispersion at E=0

  ➔ DOS, Diffusion Constant, and conductivity scaling at Weyl node

Kobayashi et.al. (2014), Syzranov et.al. (2016), Liu et.al. (2016), . . .

Scaling Theories for CI-WSM branch

Spatial anisotropic scaling

$$x'_3 = b^{\frac{1}{2}} x_3,$$
$$x'_\perp = b x_\perp,$$

with $b \equiv e^{-dl} < 1$

➔ $V' = b^{d-\frac{1}{2}} V$

with prime : After RG
Without prime : Before RG

$$N'(\mathcal{E}', \overline{\Delta}'_0, m') = b^{-(d-\frac{1}{2})} N(\mathcal{E}, \overline{\Delta}_0, m),$$

Total number of single-particle states per volume below an energy E

$$\mathcal{E}' = b^{-1}\mathcal{E},$$
$$\overline{\Delta}'_0 = b^{-y_{\overline{\Delta}}}\overline{\Delta}_0 = b^{(d-\frac{5}{2})}\overline{\Delta}_0,$$
$$m' = b^{-1} m$$

Scaling Theories for CI-WSM branch

- **Density of States:** $\rho(\mathcal{E}) \equiv \frac{dN(\mathcal{E})}{d\mathcal{E}}.$

$$\rho'(\mathcal{E}', \overline{\Delta}_0', m') = b^{-(d-\frac{1}{2}-1)} \rho(\mathcal{E}, \overline{\Delta}_0, m)$$

with $b \equiv e^{-dl} < 1$

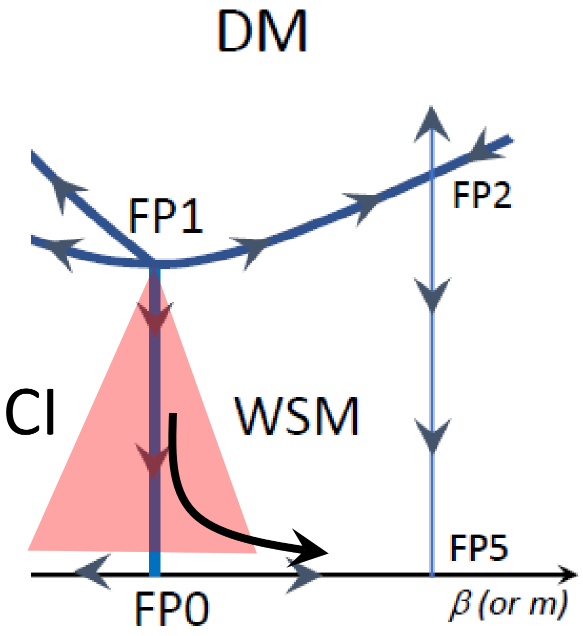

- Take *m* to be tiny, while $\overline{\Delta}_0 < \Delta_c.$
- Renormalize many times, such that $m' = b^{-y_m} m = b^{-1} m = 1$
- Solve *"b"* in favor for small *"m"*, and substitute the above equation.

$$\rho(\mathcal{E}, \overline{\Delta}_0, m) = m^{-\frac{d-\frac{1}{2}-1}{y_m}} \rho'(m^{-\frac{1}{y_m}}\mathcal{E}, m^{-\frac{y_\Delta}{y_m}}\overline{\Delta}_0, 1)$$

very small

$$\simeq m^{-\frac{d-\frac{1}{2}-1}{y_m}} \rho'(m^{-\frac{1}{y_m}}\mathcal{E}, 0, 1)$$

$$\equiv m^{-\frac{d-\frac{1}{2}-1}{y_m}} \Psi(m^{-\frac{1}{y_m}}\mathcal{E})$$

A universal Function which is encoded in FP5

$$\boxed{\rho(\mathcal{E}) = m^{-(d-\frac{3}{2})} \Psi(m^{-1}\mathcal{E})}$$

$$y_m = 1$$

Scaling Theories for CI-WSM branch

- Mean Square Displacement and diffusion constant

$$g_3(\mathcal{E}, s, \overline{\Delta}_0, m) \equiv \langle x_3^2 \rangle (\mathcal{E}, s, \overline{\Delta}_0, m),$$
$$g_\perp(\mathcal{E}, s, \overline{\Delta}_0, m) \equiv \langle x_\perp^2 \rangle (\mathcal{E}, s, \overline{\Delta}_0, m).$$

Mean Square Displacement of single-particle states of energy "$\mathcal{E}$" at a time "s" as a function of two scaling variables.

$$b^{-1} g_3'(\mathcal{E}', s', \overline{\Delta}_0', m') = g_3(\mathcal{E}, s, \overline{\Delta}_0, m),$$
$$b^{-2} g_\perp'(\mathcal{E}', s', \overline{\Delta}_0', m') = g_\perp(\mathcal{E}, s, \overline{\Delta}_0, m),$$

➔
$$g_3(\mathcal{E}, s, \overline{\Delta}_0, m) = m^{-1} \Psi_3(m^{-1}\mathcal{E}, ms),$$
$$g_\perp(\mathcal{E}, s, \overline{\Delta}_0, m) = m^{-2} \Psi_\perp(m^{-1}\mathcal{E}, ms),$$

➔
$$D_3(\mathcal{E}, \overline{\Delta}_0, m) = f_3(m^{-1}\mathcal{E}),$$
$$D_\perp(\mathcal{E}, \overline{\Delta}_0, m) = m^{-1} f_\perp(m^{-1}\mathcal{E}).$$

Universal Functions encoded in FP5

Spatial anisotropic scaling

$$x_3' = b^{\frac{1}{2}} x_3,$$
$$x_\perp' = b x_\perp,$$

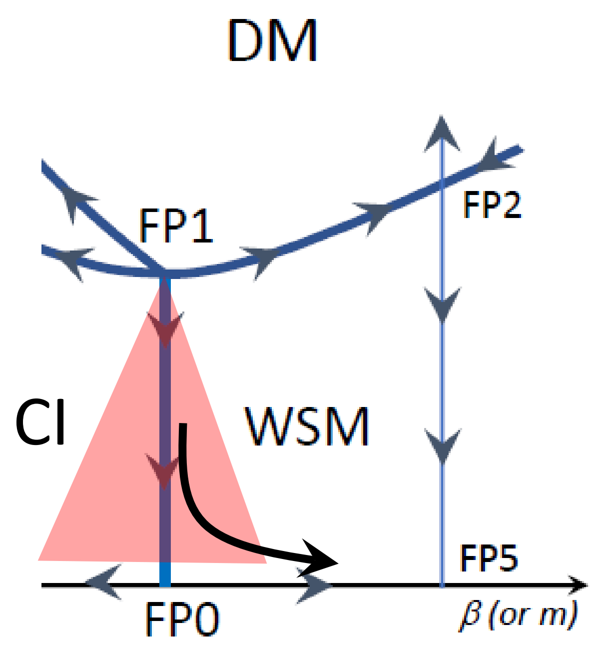

$$g_\mu(\cdots, s, \cdots) = D_\mu(\cdots)s + \mathcal{O}(s^2).$$

Linear coefficient in time "s" = Diffusion constant

□ Scaling Theories for CI-WSM branch

■ In WSM phase (m>0):

$$\boxed{\begin{aligned} &\rho(\mathcal{E}) \propto \mathcal{E}^{d-1} \\ &D_\mu(\mathcal{E}) = \frac{v_\mu^2 \tau}{3} \propto \mathcal{E}^{-(d-1)} \end{aligned}}$$

$$\boxed{\rho(\mathcal{E}) = \frac{2}{\pi \tau(\mathcal{E}) \overline{\Delta}_0}.}$$

Self-consistent Born (Liu et.al. (2016))

$$\rightarrow \begin{cases} \rho(\mathcal{E}, \overline{\Delta}_0, m) \propto m^{-\frac{1}{2}} \mathcal{E}^{d-1}, \\ D_3(\mathcal{E}, \overline{\Delta}_0, m) \propto m^{d-1} \mathcal{E}^{-(d-1)}, \\ D_\perp(\mathcal{E}, \overline{\Delta}_0, m) \propto m^{d-2} \mathcal{E}^{-(d-1)}, \\ \sigma_3(\mathcal{E}, \overline{\Delta}_0, m) \propto m^{d-\frac{3}{2}}, \\ \sigma_\perp(\mathcal{E}, \overline{\Delta}_0, m) \propto m^{d-\frac{5}{2}}, \end{cases}$$

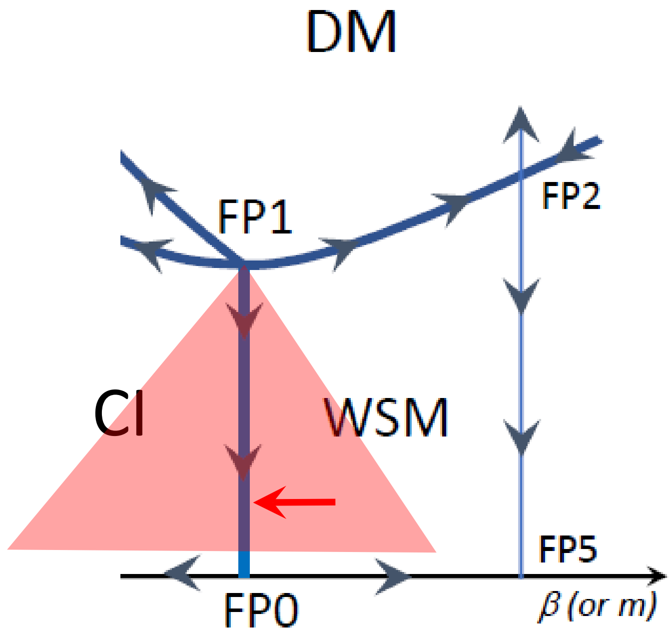

■ On a quantum critical line (m=0):

$$\boxed{\begin{aligned} &\rho(\mathcal{E}) \neq 0 \quad \text{at } \mathcal{E} \neq 0 \\ &D_\mu(\mathcal{E}) \neq 0 < +\infty \quad \text{at } \mathcal{E} \neq 0 \end{aligned}}$$

$$\rightarrow \begin{cases} \rho(\mathcal{E}, \overline{\Delta}_0, m=0) \propto \mathcal{E}^{d-\frac{3}{2}}, \\ D_3(\mathcal{E}, \overline{\Delta}_0, m=0) \propto \mathcal{E}^{0}, \\ D_\perp(\mathcal{E}, \overline{\Delta}_0, m=0) \propto \mathcal{E}^{-1}, \\ \sigma_3(\mathcal{E}, \overline{\Delta}_0, m=0) \propto \mathcal{E}^{d-\frac{3}{2}}, \\ \sigma_\perp(\mathcal{E}, \overline{\Delta}_0, m=0) \propto \mathcal{E}^{d-\frac{5}{2}}, \end{cases}$$

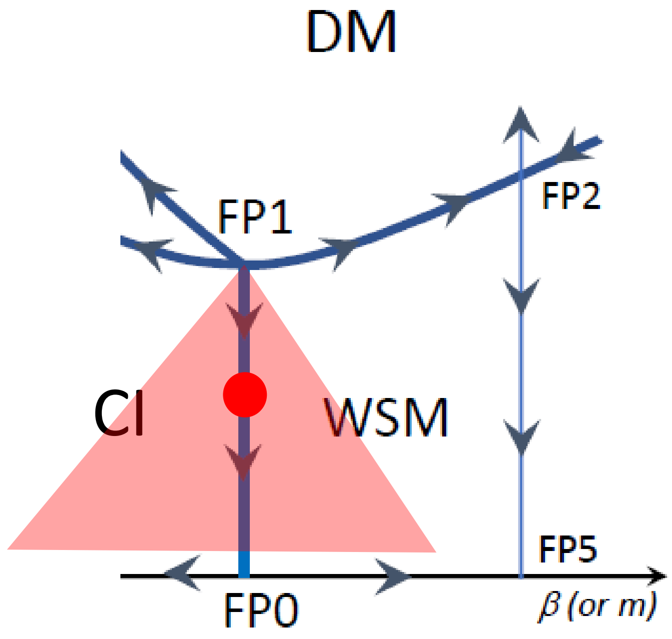

Scaling Theories around QMCP (=FP1)

$\delta\overline{\Delta}_0 \equiv \overline{\Delta}_0 - \Delta_c$, m : two relevant scaling variables

➔ two parameter scaling around QMCP

$$b^{d-\frac{1}{2}-z}\rho'(b^{-z}\mathcal{E}, b^{-y_\Delta}\delta\overline{\Delta}_0, b^{-y_m}m) = \rho(\mathcal{E}, \delta\overline{\Delta}_0, m),$$
$$b^{-1}g_3'(b^{-z}\mathcal{E}, b^z s, b^{-y_\Delta}\delta\overline{\Delta}_0, b^{-y_m}m) = g_3(\mathcal{E}, s, \delta\overline{\Delta}_0, m),$$
$$b^{-2}g_\perp'(b^{-z}\mathcal{E}, b^z s, b^{-y_\Delta}\delta\overline{\Delta}_0, b^{-y_m}m) = g_\perp(\mathcal{E}, s, \delta\overline{\Delta}_0, m),$$

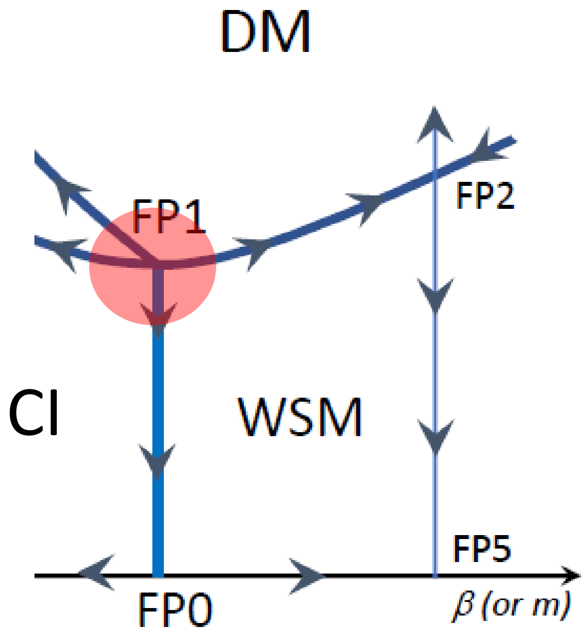

z, y_Δ, y_m :Dynamical exponents, scaling dimensions at QMCP (=FP1)

$$z = 1 + \frac{1}{n} + \mathcal{O}(n^{-2}), \quad y_m = 1 - \frac{1}{n} + \mathcal{O}(n^{-2}), \quad y_\Delta = \frac{1}{n} + \mathcal{O}(n^{-2})$$

■ Approaching QMCP along *m=0*

$$\begin{cases} \rho(\mathcal{E}, \delta\overline{\Delta}_0) = |\delta\overline{\Delta}_0|^{\frac{d-\frac{1}{2}-z}{y_\Delta}} \Psi(|\delta\overline{\Delta}_0|^{-\frac{z}{y_\Delta}}\mathcal{E}), \\ D_3(\mathcal{E}, \delta\overline{\Delta}_0) = |\delta\overline{\Delta}_0|^{\frac{z-1}{y_\Delta}} f_z(|\delta\overline{\Delta}_0|^{-\frac{z}{y_\Delta}}\mathcal{E}), \\ D_\perp(\mathcal{E}, \delta\overline{\Delta}_0) = |\delta\overline{\Delta}_0|^{\frac{z-2}{y_\Delta}} f_\perp(|\delta\overline{\Delta}_0|^{-\frac{z}{y_\Delta}}\mathcal{E}). \end{cases}$$

$$|m| \ll A|\delta\overline{\Delta}_0|^{\frac{y_m}{y_\Delta}}$$

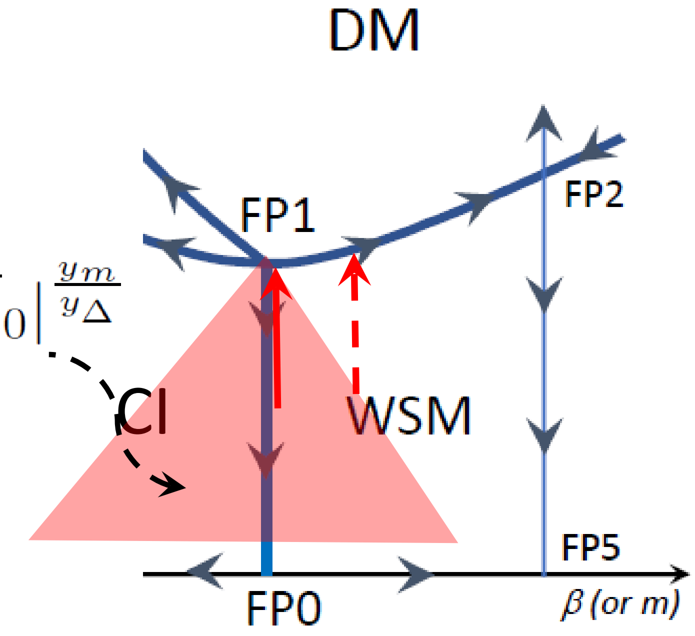

Crossover boundary: $\begin{cases} |m| \ll A|\delta\overline{\Delta}_0|^{\frac{y_m}{y_\Delta}} & : \text{controlled by FP1} \\ |m| \gg A|\delta\overline{\Delta}_0|^{\frac{y_m}{y_\Delta}} & : \text{controlled by FP2, 3, 4} \end{cases}$

Scaling Theories around QMCP (=FP1)

- Approaching QMCP along *m=0*

$$\left\{\begin{array}{c} \rho(\mathcal{E}) \propto |\mathcal{E}|^{d-\frac{3}{2}}, \\ D_3(\mathcal{E}) \propto |\mathcal{E}|^{0}, \\ D_\perp(\mathcal{E}) \propto |\mathcal{E}|^{-1}. \end{array}\right. + \left\{\begin{array}{c} \rho(\mathcal{E},\delta\overline{\Delta}_0) = |\delta\overline{\Delta}_0|^{\frac{d-\frac{1}{2}-z}{y_\Delta}}\Psi(|\delta\overline{\Delta}_0|^{-\frac{z}{y_\Delta}}\mathcal{E}), \\ D_3(\mathcal{E},\delta\overline{\Delta}_0) = |\delta\overline{\Delta}_0|^{\frac{z-1}{y_\Delta}} f_z(|\delta\overline{\Delta}_0|^{-\frac{z}{y_\Delta}}\mathcal{E}), \\ D_\perp(\mathcal{E},\delta\overline{\Delta}_0) = |\delta\overline{\Delta}_0|^{\frac{z-2}{y_\Delta}} f_\perp(|\delta\overline{\Delta}_0|^{-\frac{z}{y_\Delta}}\mathcal{E}). \end{array}\right. \rightarrow \left\{\begin{array}{c} \rho(\mathcal{E}) \propto |\delta\overline{\Delta}_0|^{\frac{2d-1}{2}\frac{1-z}{y_\Delta}}|\mathcal{E}|^{d-\frac{3}{2}}, \\ D_3(\mathcal{E}) \propto |\delta\overline{\Delta}_0|^{\frac{z-1}{y_\Delta}}|\mathcal{E}|^{0}, \\ D_\perp(\mathcal{E}) \propto |\delta\overline{\Delta}_0|^{\frac{2(z-1)}{y_\Delta}}|\mathcal{E}|^{-1}, \\ \sigma_3(\mathcal{E}) \propto |\delta\overline{\Delta}_0|^{\frac{2d-3}{2}\frac{1-z}{y_\Delta}}|\mathcal{E}|^{d-\frac{3}{2}}, \\ \sigma_\perp(\mathcal{E}) \propto |\delta\overline{\Delta}_0|^{\frac{2d-5}{2}\frac{1-z}{y_\Delta}}|\mathcal{E}|^{d-\frac{5}{2}}. \end{array}\right.$$

Determined by FP0 **Determined by FP1**

$$\left\{\begin{array}{c} \rho(\mathcal{E},\overline{\Delta}_0,m=0) \propto \mathcal{E}^{d-\frac{3}{2}}, \\ D_3(\mathcal{E},\overline{\Delta}_0,m=0) \propto \mathcal{E}^{0}, \\ D_\perp(\mathcal{E},\overline{\Delta}_0,m=0) \propto \mathcal{E}^{-1}, \\ \sigma_3(\mathcal{E},\overline{\Delta}_0,m=0) \propto \mathcal{E}^{d-\frac{3}{2}}, \\ \sigma_\perp(\mathcal{E},\overline{\Delta}_0,m=0) \propto \mathcal{E}^{d-\frac{5}{2}}, \end{array}\right.$$

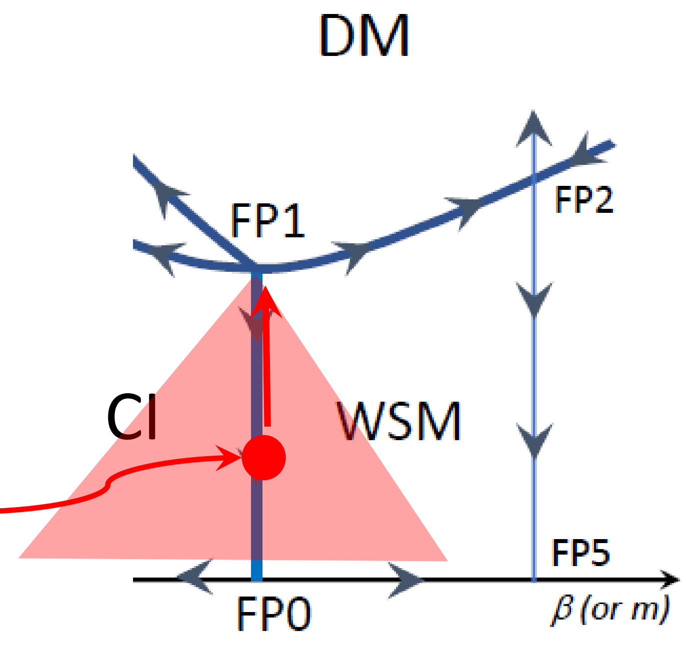

Scaling Theories around QMCP (=FP1)

Approaching QMCP along $\delta\Delta_0$=0

$$\begin{cases} \rho(\mathcal{E}, \delta\overline{\Delta}_0 = 0, m) \propto |\mathcal{E}|^{\frac{d-z'}{z'}}, \\ D(\mathcal{E}, \delta\overline{\Delta}_0 = 0, m) \propto |\mathcal{E}|^{\frac{z'-2}{z'}}, \\ \sigma(\mathcal{E}, \delta\overline{\Delta}_0 = 0, m) \propto |\mathcal{E}|^{\frac{d-2}{z'}}. \end{cases} + \begin{cases} \rho(\mathcal{E}, m) = |m|^{\frac{d-\frac{1}{2}-z}{y_m}} \Psi(|m|^{-\frac{z}{y_m}}\mathcal{E}), \\ D_3(\mathcal{E}, m) = |m|^{\frac{z-1}{y_m}} f_z(|m|^{-\frac{z}{y_m}}\mathcal{E}), \\ D_\perp(\mathcal{E}, m) = |m|^{\frac{z-2}{y_m}} f_\perp(|m|^{-\frac{z}{y_m}}\mathcal{E}), \end{cases}$$

Determined by FP2 **Determined by FP1**

$$\rightarrow \begin{cases} \rho(\mathcal{E}, \delta\overline{\Delta}_0 = 0, m) \propto m^{\frac{1}{2y_m}\left(2d\frac{z'-z}{z'}-1\right)} |\mathcal{E}|^{\frac{d-z'}{z'}}, \\ D_3(\mathcal{E}, \delta\overline{\Delta}_0 = 0, m) \propto m^{\frac{1}{y_m}\left(\frac{2z}{z'}-1\right)} |\mathcal{E}|^{\frac{z'-2}{z'}}, \\ D_\perp(\mathcal{E}, \delta\overline{\Delta}_0 = 0, m) \propto m^{\frac{2}{y_m}\left(\frac{z}{z'}-1\right)} |\mathcal{E}|^{\frac{z'-2}{z'}}, \text{ (D} \\ \sigma_3(\mathcal{E}, \delta\overline{\Delta}_0 = 0, m) \propto m^{\frac{1}{y_m}\left(d-\frac{z}{z'}(d-2)-\frac{3}{2}\right)} |\mathcal{E}|^{\frac{d-2}{z'}}, \\ \sigma_\perp(\mathcal{E}, \delta\overline{\Delta}_0 = 0, m) \propto m^{\frac{1}{y_m}\left(d-\frac{z}{z'}(d-2)-\frac{5}{2}\right)} |\mathcal{E}|^{\frac{d-2}{z'}}. \end{cases}$$

z' :Dynamical exponents around FP2 (=Fradkin's fixed point)

z' =d/2 + ….

Syzranov et.al. (2016), Roy et.al. (2014,2016), ..
Kobayashi et.al.(2014), Liu et.al. (2016), …

$$\begin{cases} \rho(\mathcal{E}, \delta\overline{\Delta}_0 = 0, m) \propto |\mathcal{E}|^{\frac{d-z'}{z'}}, \\ D(\mathcal{E}, \delta\overline{\Delta}_0 = 0, m) \propto |\mathcal{E}|^{\frac{z'-2}{z'}}, \\ \sigma(\mathcal{E}, \delta\overline{\Delta}_0 = 0, m) \propto |\mathcal{E}|^{\frac{d-2}{z'}}. \end{cases}$$

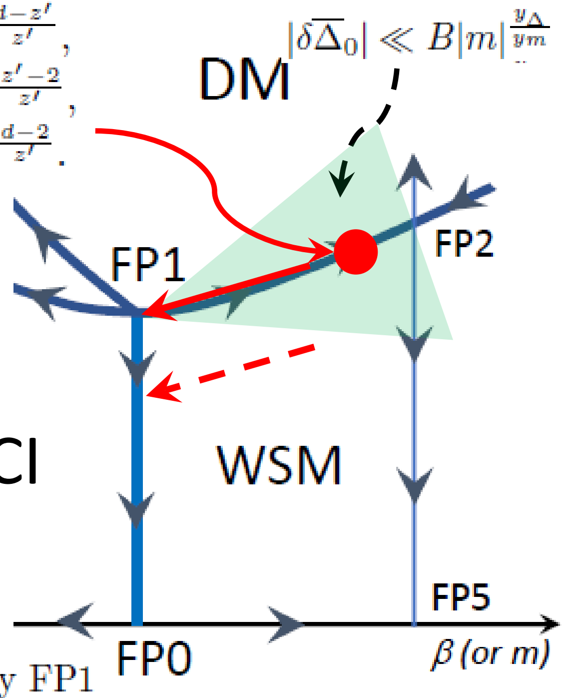

On QMCP at $\delta\Delta_0$=0, m=0

$$\begin{cases} \rho(\mathcal{E}) \propto |\mathcal{E}|^{\frac{d-\frac{1}{2}-z}{z}}, \\ D_z(\mathcal{E}) \propto |\mathcal{E}|^{\frac{z-1}{z}}, \\ D_\perp(\mathcal{E}) \propto |\mathcal{E}|^{\frac{z-2}{z}}. \end{cases}$$

Determined only by dynamical Exponent at FP1, anisotropic in space.

Crossover boundary:

$$\begin{cases} |\delta\overline{\Delta}_0| \ll B|m|^{\frac{y_\Delta}{y_m}} & \text{: controlled by FP1} \\ |\delta\overline{\Delta}_0| \gg B|m|^{\frac{y_\Delta}{y_m}} & \text{: controlled by FP0} \end{cases}$$

◻ effective velocities, and life time in WSM, on QMCP, critical line between CI and WSM and that between DM and WSM.

- Diffusion constant
  ← velocities and life time

$$D_\mu(\mathcal{E}) = v_\mu^2 \tau(\mathcal{E}),$$

- DOS ← velocities

E.g. $\rho(\mathcal{E}) = v_3^{-1} v_\perp^{-2} |\mathcal{E}|^{d-1}$

	$\rho(0)$ or $\rho(\mathcal{E})$	$D_3(0)$ or $D_3(\mathcal{E})$	$D_\perp(0)$ or $D_\perp(\mathcal{E})$	$v_3(0)$ or $v_3(\mathcal{E})$	$v_\perp(0)$ or $v_\perp(\mathcal{E})$	$\tau(0)$ or $\tau(\mathcal{E})$
(i)	$\lvert\delta\overline{\Delta}_0\rvert^{\frac{2d-1-2z}{2y_\Delta}}$	$\lvert\delta\overline{\Delta}_0\rvert^{\frac{z-1}{y_\Delta}}$	$\lvert\delta\overline{\Delta}_0\rvert^{\frac{z-2}{y_\Delta}}$	—	—	$\rho^{-1}(0)$
(ii)	$\mathcal{E}^{d-\frac{3}{2}}$	$\neq 0$	$\mathcal{E}^{-1}$	$\mathcal{E}^{\frac{1}{2}}$	$\neq 0$	$\mathcal{E}^{-1}$
(ii)′	$\lvert\delta\overline{\Delta}_0\rvert^{\frac{2d-1}{2}\frac{1-z}{y_\Delta}}\mathcal{E}^{d-\frac{3}{2}}$	$\lvert\delta\overline{\Delta}_0\rvert^{\frac{z-1}{y_\Delta}}$	$\lvert\delta\overline{\Delta}_0\rvert^{\frac{2(z-1)}{y_\Delta}}\mathcal{E}^{-1}$	$\lvert\delta\overline{\Delta}_0\rvert^{\frac{1}{2}\frac{z-1}{y_\Delta}}\mathcal{E}^{\frac{1}{2}}$	$\lvert\delta\overline{\Delta}_0\rvert^{\frac{z-1}{y_\Delta}}$	$\mathcal{E}^{-1}$
(iii)	$\mathcal{E}^{\frac{d-z'}{z'}}$	$\mathcal{E}^{\frac{z'-2}{z'}}$		$\mathcal{E}^{\frac{z'-1}{z'}}$		$\mathcal{E}^{-1}$
(iii)′	$\lvert m\rvert^{\frac{2d(z'-z)-z'}{2z'y_m}}\mathcal{E}^{\frac{d-z'}{z'}}$	$\lvert m\rvert^{\frac{2z-z'}{z'y_m}}\mathcal{E}^{\frac{z'-2}{z'}}$	$\lvert m\rvert^{\frac{2(z-z')}{z'y_m}}\mathcal{E}^{\frac{z'-2}{z'}}$	$\lvert m\rvert^{\frac{1}{2}\frac{2z-z'}{z'y_m}}\mathcal{E}^{\frac{z'-1}{z'}}$	$\lvert m\rvert^{\frac{z-z'}{z'y_m}}\mathcal{E}^{\frac{z'-1}{z'}}$	$\mathcal{E}^{-1}$
(iv)	$\mathcal{E}^{\frac{2d-1-2z}{2z}}$	$\mathcal{E}^{\frac{z-1}{z}}$	$\mathcal{E}^{\frac{z-2}{z}}$	$\mathcal{E}^{\frac{2z-1}{2z}}$	$\mathcal{E}^{\frac{z-1}{z}}$	$\mathcal{E}^{-1}$
(vii)	$\lvert m\rvert^{-\frac{1}{2}}\mathcal{E}^{d-1}$	$\lvert m\rvert^{d-1}\mathcal{E}^{-(d-1)}$	$\lvert m\rvert^{d-2}\mathcal{E}^{-(d-1)}$	$\lvert m\rvert^{\frac{1}{2}}$	$\neq 0$	$m^{d-2}\mathcal{E}^{-(d-1)}$

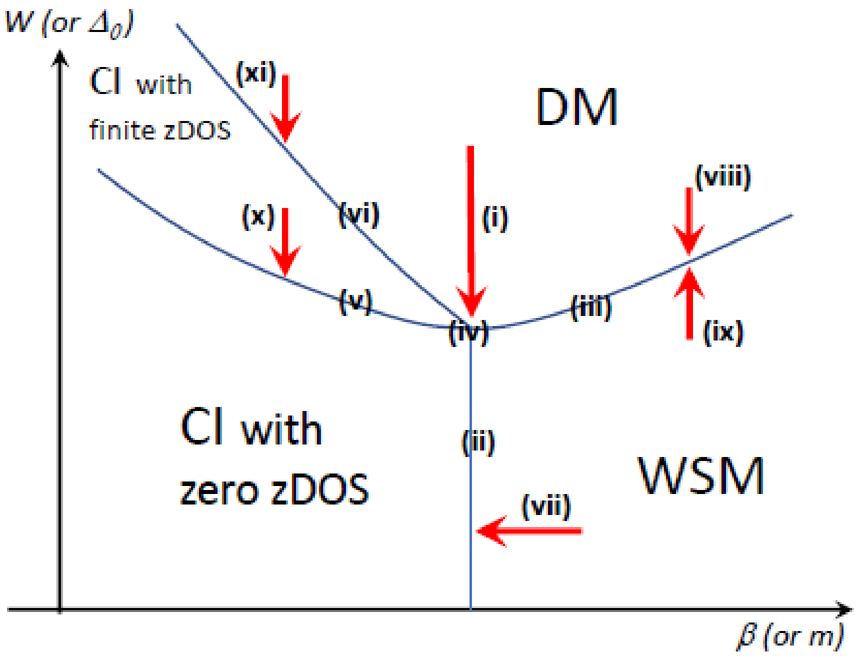

- Effective velocities also shows strong spatial anisotropy
- life time in two quantum critical lines as well as QMCP is always scaled as E^{-1}

$$\sigma_\mu = e^2 \rho D_\mu \quad \text{(Einstein Relation)}$$

	$\rho(0)$ or $\rho(\mathcal{E})$	$\sigma_3(0)$ or $\sigma_3(\mathcal{E})$	$\sigma_\perp(0)$ or $\sigma_\perp(\mathcal{E})$
(i)	$\delta\overline{\Delta}_0^{\frac{2d-1-2z}{2y_\Delta}}$	$\delta\overline{\Delta}_0^{\frac{2d-3}{2y_\Delta}}$	$\delta\overline{\Delta}_0^{\frac{2d-5}{2y_\Delta}}$
(ii)	$\lvert\mathcal{E}\rvert^{d-\frac{3}{2}}$	$\lvert\mathcal{E}\rvert^{d-\frac{3}{2}}$	$\lvert\mathcal{E}\rvert^{d-\frac{5}{2}}$
(ii)′	$\lvert\delta\overline{\Delta}_0\rvert^{\frac{2d-1}{2}\frac{1-z}{y_\Delta}}\lvert\mathcal{E}\rvert^{d-\frac{3}{2}}$	$\lvert\delta\overline{\Delta}_0\rvert^{\frac{2d-3}{2}\frac{1-z}{y_\Delta}}\lvert\mathcal{E}\rvert^{d-\frac{3}{2}}$	$\lvert\delta\overline{\Delta}_0\rvert^{\frac{2d-5}{2}\frac{1-z}{y_\Delta}}\lvert\mathcal{E}\rvert^{d-\frac{5}{2}}$
(iii)	$\lvert\mathcal{E}\rvert^{\frac{d-z'}{z'}}$	$\lvert\mathcal{E}\rvert^{\frac{d-2}{z'}}$	same as σ_3
(iii)′	$m^{\frac{2d(z'-z)-z'}{2z'y_m}}\lvert\mathcal{E}\rvert^{\frac{d-z'}{z'}}$	$m^{\frac{2d(z'-z)+4z-3z'}{2z'y_m}}\lvert\mathcal{E}\rvert^{\frac{d-2}{z'}}$	$m^{\frac{2d(z'-z)+4z-5z'}{2z'y_m}}\lvert\mathcal{E}\rvert^{\frac{d-2}{z'}}$
(iv)	$\lvert\mathcal{E}\rvert^{\frac{2d-1-2z}{2z}}$	$\lvert\mathcal{E}\rvert^{\frac{2d-3}{2z}}$	$\lvert\mathcal{E}\rvert^{\frac{2d-5}{2z}}$
(vii)	$m^{-\frac{1}{2}}\lvert\mathcal{E}\rvert^{d-1}$	$m^{d-\frac{3}{2}}$	$m^{d-\frac{5}{2}}$

Nature of phase transitions from CI phase to DM phase

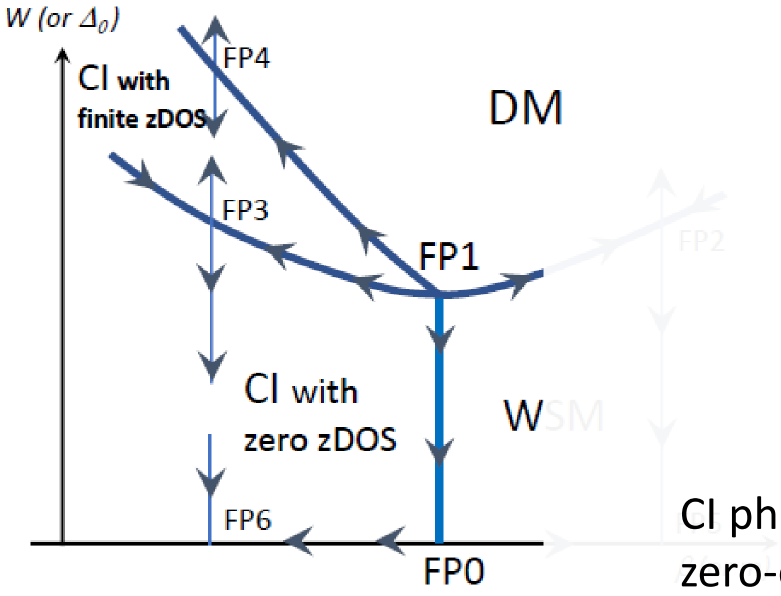

Diffusive metal (DM) phase

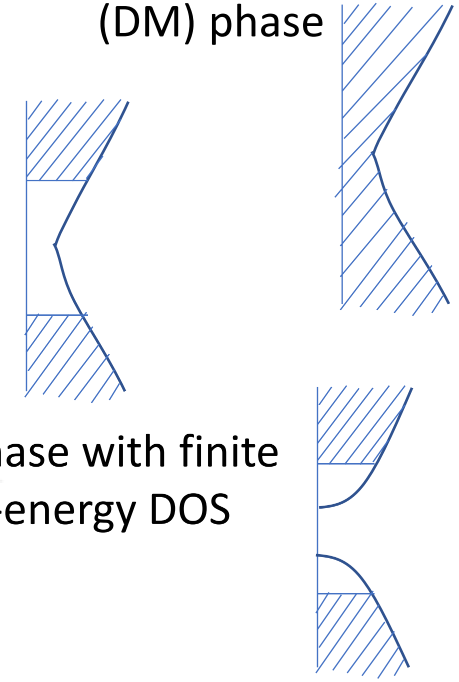

CI phase with finite zero-energy DOS

CI phase with zero zero-energy DOS

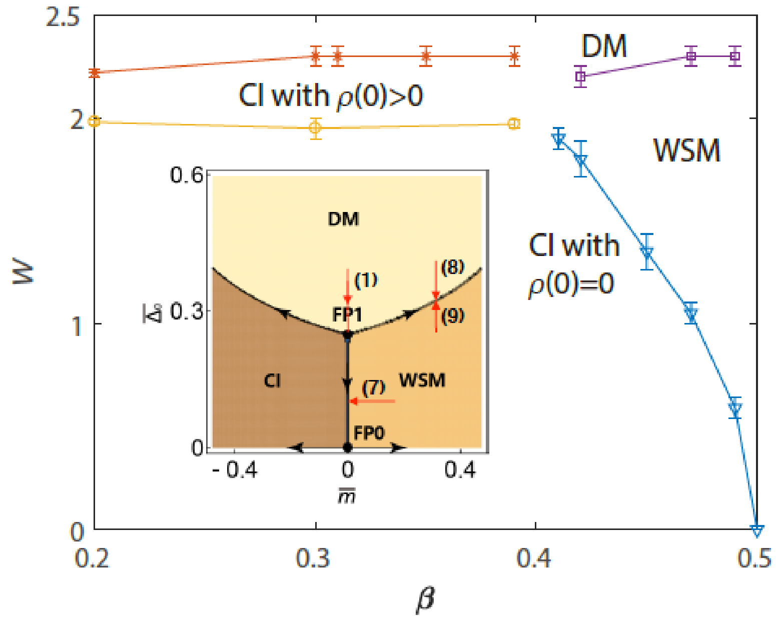

◆ Localization length (transfer matrix method)

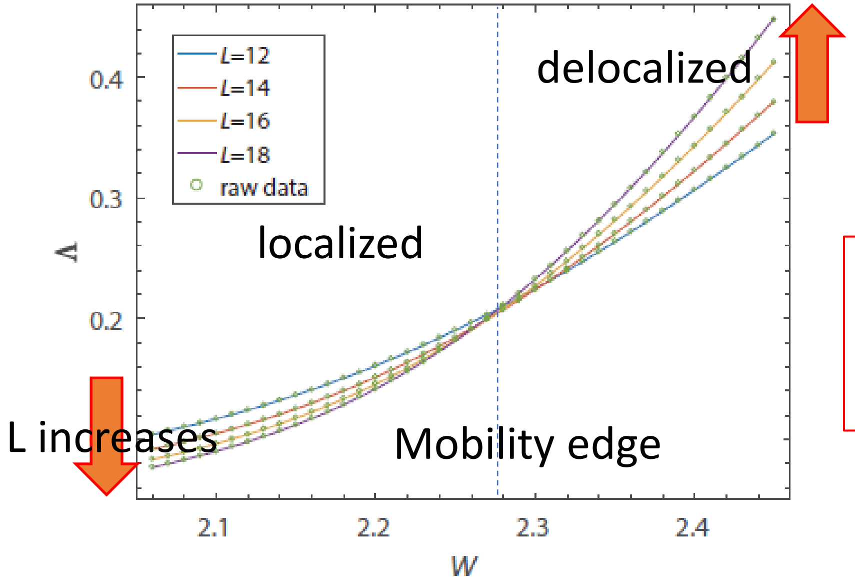

■ For CI-DM branch,
Mobility edge and band edge
are distinct in the phase diagram

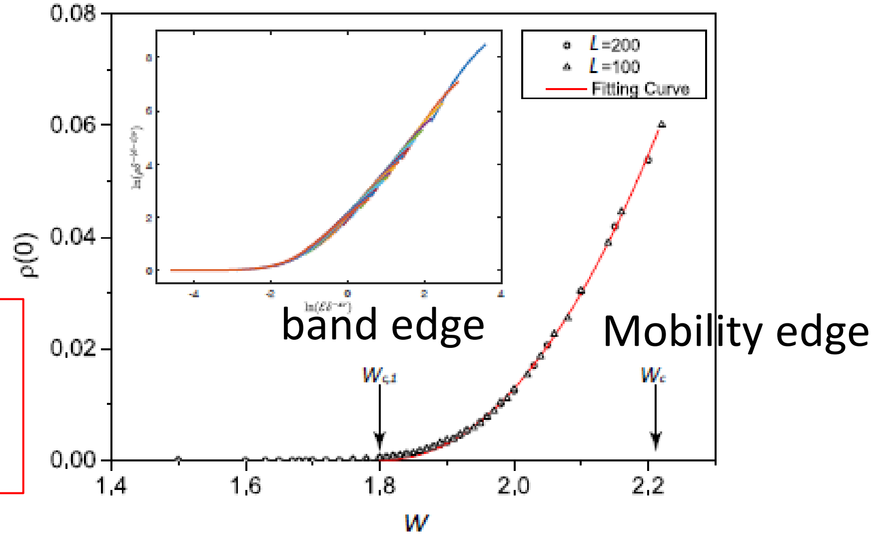

◆ Zero-energy Density of states (Kernel Polynomial)

Criticality at mobility edge between CI phase with finite zDOS and DM phase

◆ Finite-size scaling analysis (Polynonial Fitting results)

m_1	m_2	GOF	W_c	ν	$-y$
2	0	0.27	2.21[2.19,2.23]	1.34[1.23,1.53]	2.6[2.0,3.4]
3	0	0.82	2.22[2.18,2.23]	1.27[1.18,1.48]	3.0[2.0,4.0]
2	1	0.29	2.22[2.19,2.23]	1.31[1.22,1.52]	3.0[2.1,3.9]
3	1	0.81	2.22[2.18,2.23]	1.26[1.18,1.48]	2.9[2.0,3.8]

Consistent with value of exponent in 3D unitary class

ν=1.44* : **3D unitary class**

Slevin-Ohtsuki (2016)

● Finite DOS → dynamical exponent z=d

$$\rho(\mathcal{E}) = \xi^{(d-z)\nu}\Psi(\xi^{-z\nu}\mathcal{E})$$

■ Criticality at the mobility edge in CI-DM branch belongs to conventional 3D unitary class with z=3

◆ Distribution of Conductance at the critical point (CCD; critical conductance distribution)

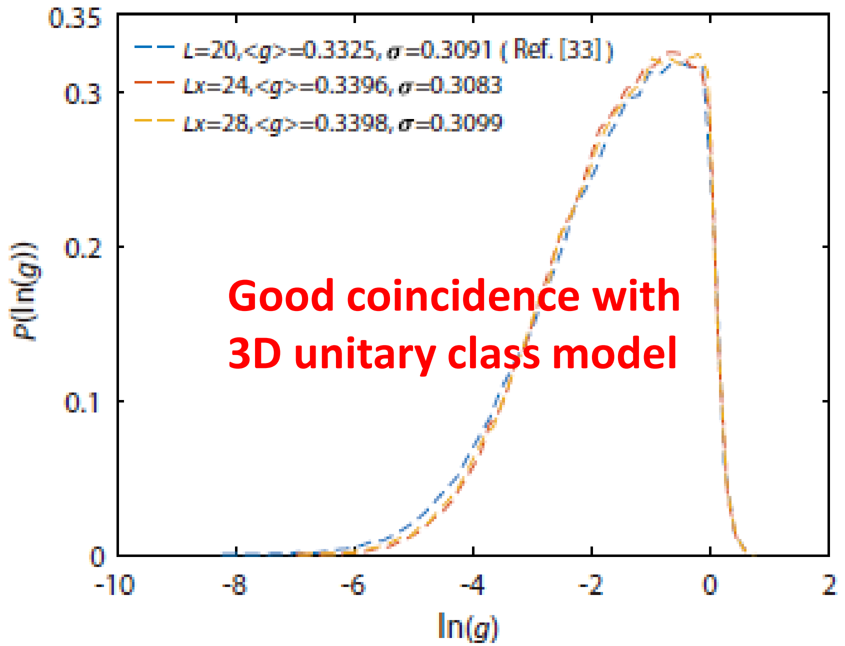

● CCD generally depends only on universality class and system geometry, but free from the system size (scale-invariance at the critical point).

● Compare with CCD of a reference tight-binding model whose Anderson transition is known to belong to conventional 3D unitary class.

Criticality at the band edge for CI-DM branch

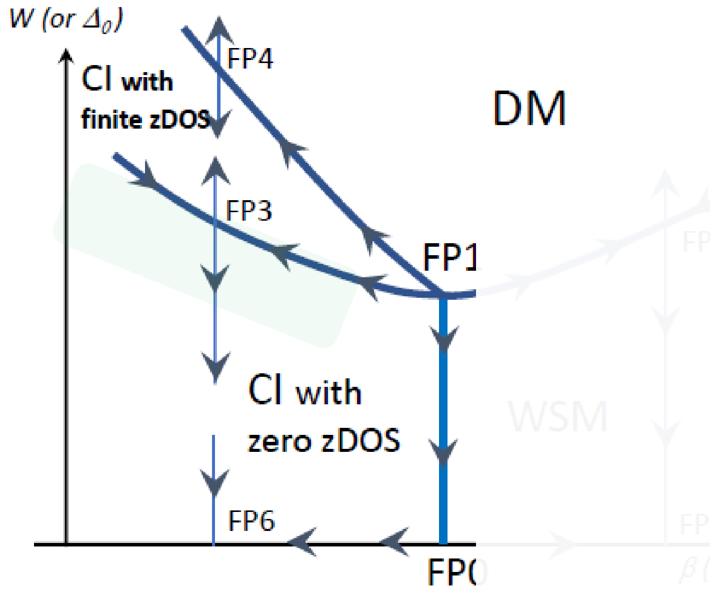

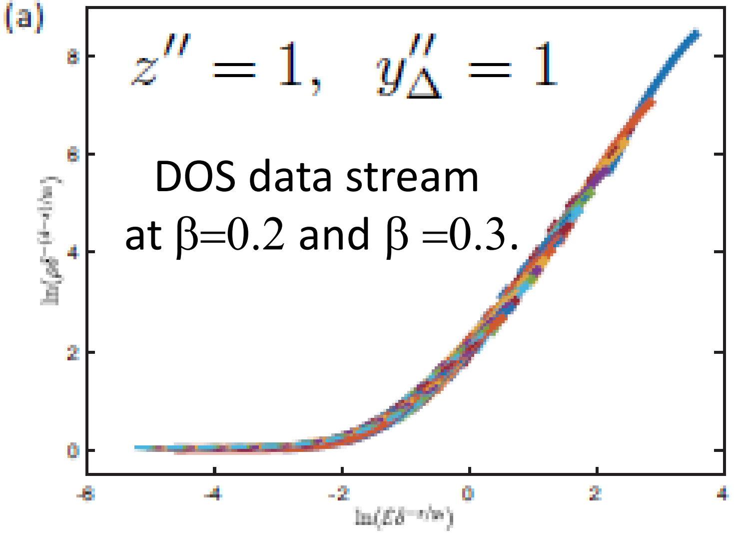

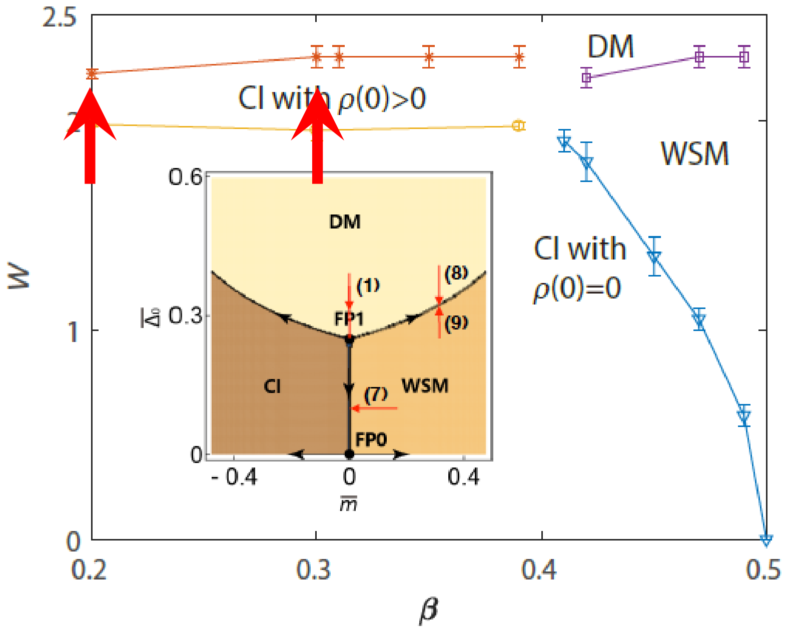

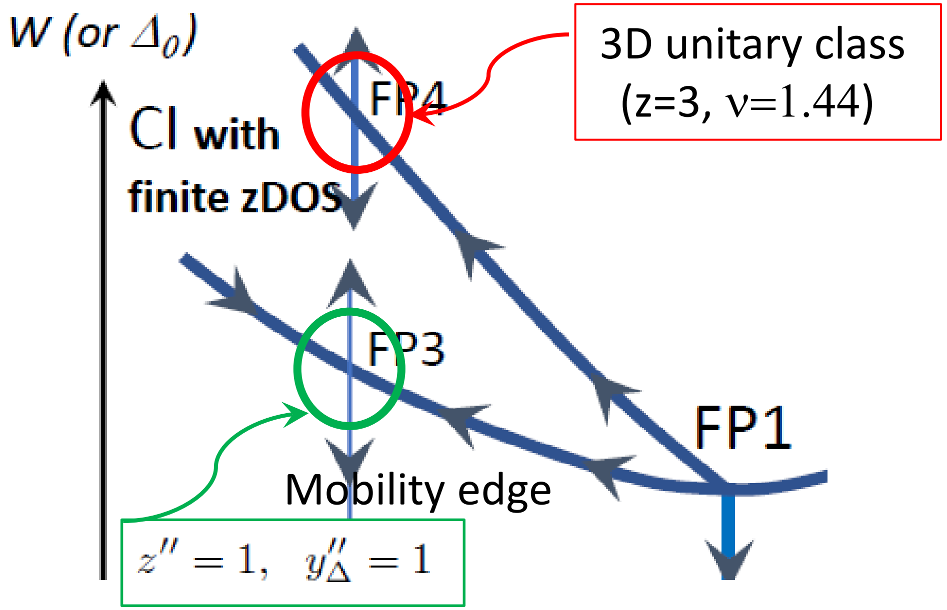

$$\rho(\mathcal{E}, \delta\overline{\Delta}_0, m) = |\delta\overline{\Delta}_0|^{\frac{d-z''}{y''_{\Delta}}} \Psi\left(|\delta\overline{\Delta}_0|^{-\frac{z''}{y''_{\Delta}}} \mathcal{E}\right),$$

◆ DOS data for different β (or m) are fit into a single-parameter scaling function !!

$$\rho(\mathcal{E}, W, \beta) = \left(a(\beta)|W - W_c(\beta)|\right)^{-\frac{z-d}{y_t}} \times \Phi\left(\left(a(\beta)|W - W_c(\beta)|\right)^{-\frac{z}{y_t}} \mathcal{E}\right),$$

$$\rightarrow \quad z'' = 1, \quad y''_{\Delta} = 1$$

Summary (Disorder-driven quantum phase transition in WSM)

- Novel disorder-driven Quantum multicriticality (QMC)
  - Rich scaling properties of DOS, conductivity, and diffusion constant around Weyl nodes

Luo, Xu, Ohtsuki and RS, ArXiv:1710.00572v2

- Spatially anisotropic scalings in QMCP and critical line between CI and WSM phases

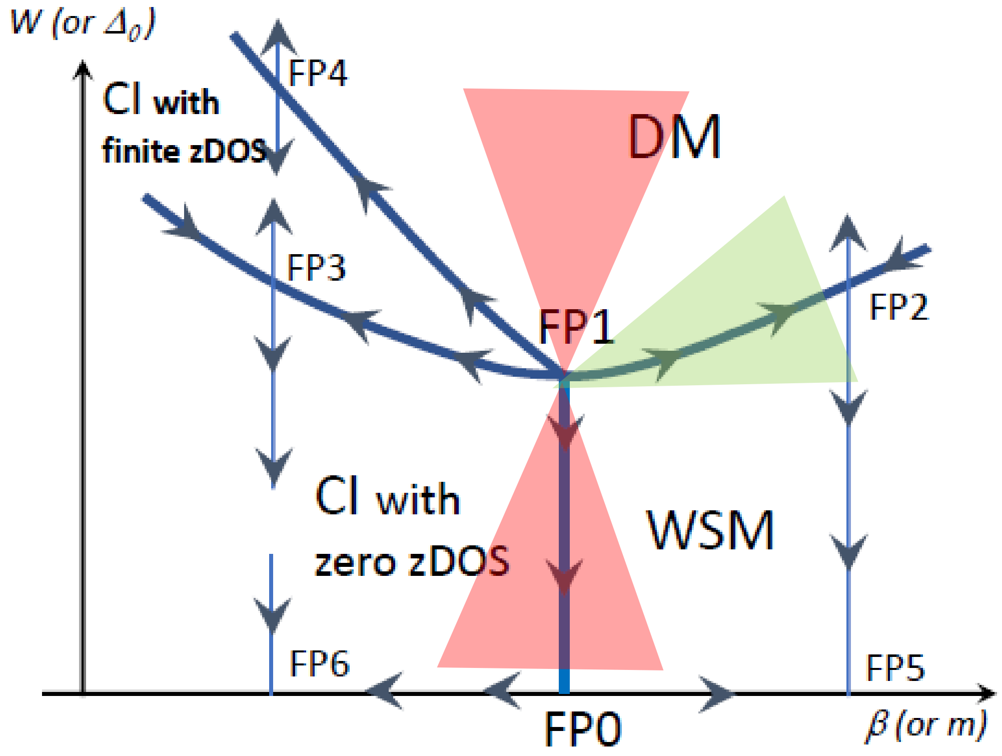

- New fixed points other than Fradkin's fixed point

	$\rho(0)$ or $\rho(\mathcal{E})$	$\sigma_3(0)$ or $\sigma_3(\mathcal{E})$	$\sigma_\perp(0)$ or $\sigma_\perp(\mathcal{E})$
(i)	$\delta\overline{\Delta}_0^{\frac{2d-1-2z}{2y_\Delta}}$	$\delta\overline{\Delta}_0^{\frac{2d-3}{2y_\Delta}}$	$\delta\overline{\Delta}_0^{\frac{2d-5}{2y_\Delta}}$
(ii)	$\lvert\mathcal{E}\rvert^{d-\frac{3}{2}}$	$\lvert\mathcal{E}\rvert^{d-\frac{3}{2}}$	$\lvert\mathcal{E}\rvert^{d-\frac{5}{2}}$
(ii)'	$\lvert\delta\overline{\Delta}_0\rvert^{\frac{2d-1}{2}\frac{1-z}{y_\Delta}}\lvert\mathcal{E}\rvert^{d-\frac{3}{2}}$	$\lvert\delta\overline{\Delta}_0\rvert^{\frac{2d-3}{2}\frac{1-z}{y_\Delta}}\lvert\mathcal{E}\rvert^{d-\frac{3}{2}}$	$\lvert\delta\overline{\Delta}_0\rvert^{\frac{2d-5}{2}\frac{1-z}{y_\Delta}}\lvert\mathcal{E}\rvert^{d-\frac{5}{2}}$
(iii)	$\lvert\mathcal{E}\rvert^{\frac{d-z'}{z'}}$	$\lvert\mathcal{E}\rvert^{\frac{d-2}{z'}}$	same as σ_3
(iii)'	$m^{\frac{2d(z'-z)-z'}{2z'y_m}}\lvert\mathcal{E}\rvert^{\frac{d-z'}{z'}}$	$m^{\frac{2d(z'-z)+4z-3z'}{2z'y_m}}\lvert\mathcal{E}\rvert^{\frac{d-2}{z'}}$	$m^{\frac{2d(z'-z)+4z-5z'}{2z'y_m}}\lvert\mathcal{E}\rvert^{\frac{d-2}{z'}}$
(iv)	$\lvert\mathcal{E}\rvert^{\frac{2d-1-2z}{2z}}$	$\lvert\mathcal{E}\rvert^{\frac{2d-3}{2z}}$	$\lvert\mathcal{E}\rvert^{\frac{2d-5}{2z}}$
(vii)	$m^{-\frac{1}{2}}\lvert\mathcal{E}\rvert^{d-1}$	$m^{d-\frac{3}{2}}$	$m^{d-\frac{5}{2}}$

Content

- ☐ Disorder-driven quantum phase transition in Weyl fermion semimetal
  - ■ Quantum multicriticality with spatially anisotropic scaling
  - ■ DOS, conductivity, and diffusion constant scalings near Weyl nodes
  - ■ Unconventional critical exponent associated with 3D band insulator-Weyl semimetal transition

- ☐ **Correlation-driven metal-insulator transition in graphite under H**

Zhang and RS, Phys. Rev. B 95, 205108 (2017)

Pan and RS, in preparation

Zhiming Pan (PKU), Xiaotian Zhang (PKU), Ryuichi Shindou (PKU)

☐ Experimental `Example' of magnetic Weyl semimetal

: 3D metal/semimetal under high magnetic field

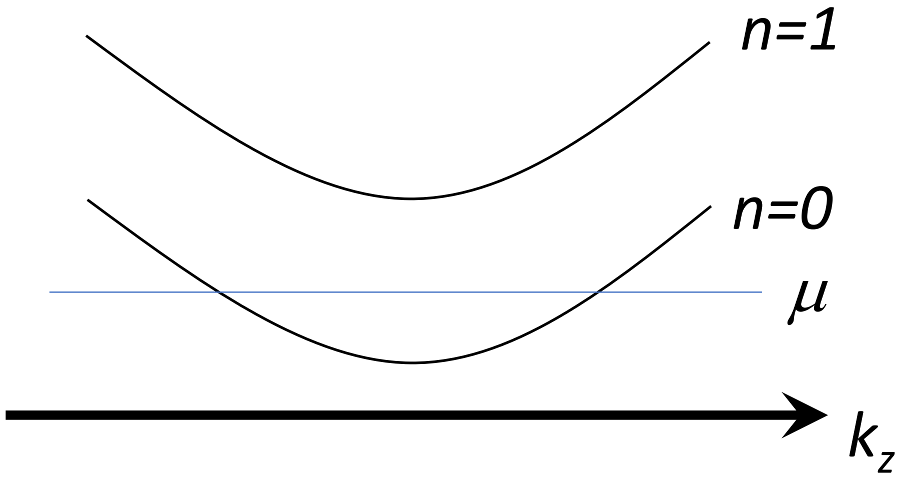

$$\mathcal{H}_{\mathrm{kin}} = \int d\boldsymbol{r}\, \Psi^{\dagger}(\boldsymbol{r}) \left(\frac{\boldsymbol{\pi}^2}{2m_*} - \mu \right) \Psi(\boldsymbol{r})$$

$$= \sum_{n,k_z,j} \left[\frac{\hbar^2 k_z^2}{2m_*} + \left(n + \frac{1}{2}\right)\hbar\omega_0 - \mu \right] c^{\dagger}_{n,j,k_z} c_{n,j,k_z},$$

- "j" specifies a location of a single-particle eigenstate localized along y-direction (y_j) and momentum along x-direction (k_x)

$$k_x \equiv 2\pi j/L_x \quad y_j \equiv 2\pi l^2 j/L_x$$

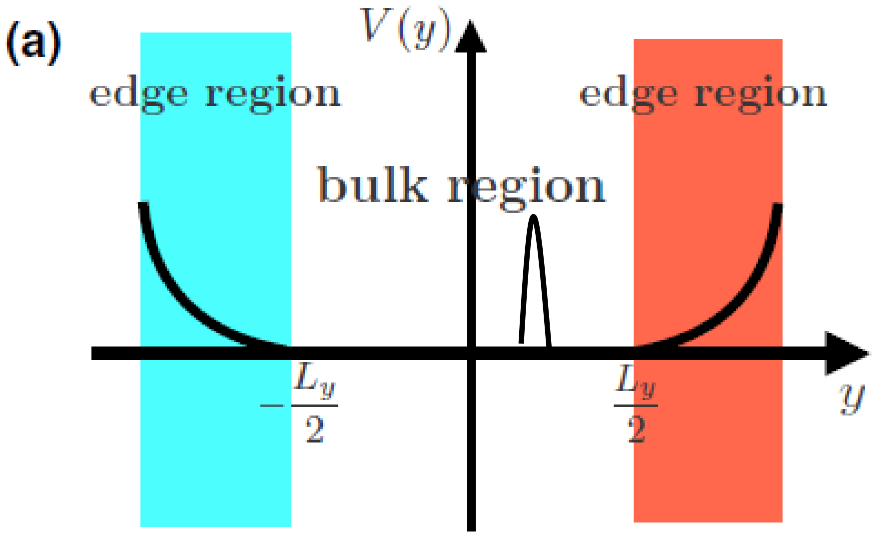

- confining potential V(x) around the boundaries
- When magnetic length l << $|dV/dx|^{-1}$

$$E = \frac{\hbar^2 k_z^2}{2m_*} + \left(n + \frac{1}{2}\right)\hbar\omega_0 + V(k_x l^2)$$

□ Experimental `Example' of magnetic Weyl semimetal
: 3D metal/semimetal under high magnetic field

- When magnetic length l << |dV/dx|$^{-1}$ Halperin (1982, 1985)

$$E = \frac{\hbar^2 k_z^2}{2m_*} + \left(n + \frac{1}{2}\right)\hbar\omega_0 + V(k_x l^2)$$

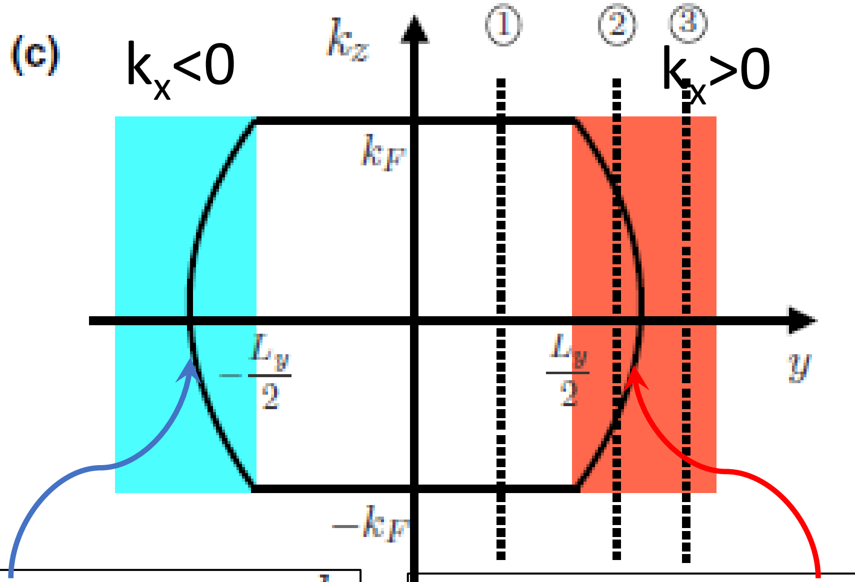

Localized at x=-L_y/2, positive momentum along x-direction

Localized at x=L_y/2, positive momentum along x-direction

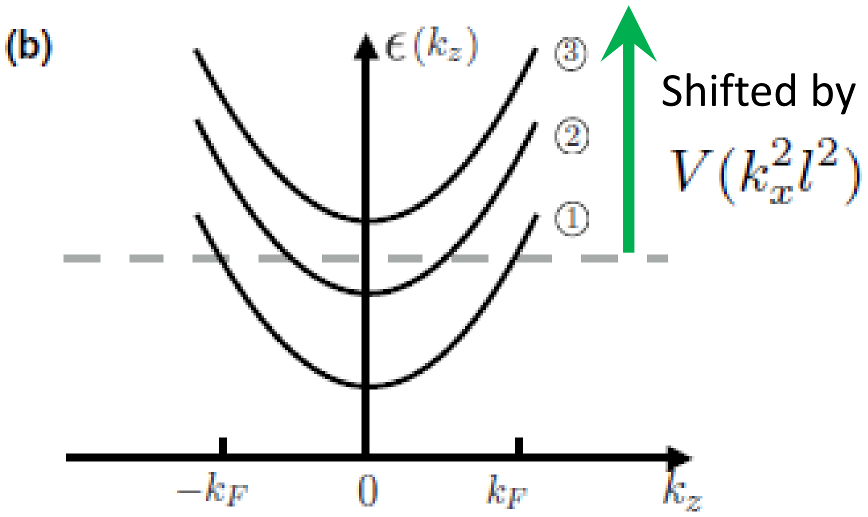

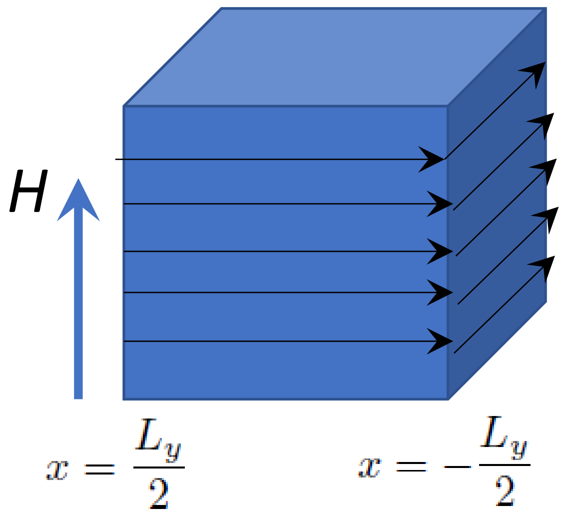

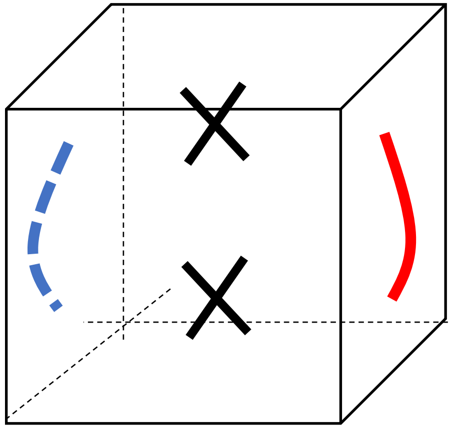

"Surface chiral Fermi arc (SCFA) state"

Peierls Instability in 3D metal/semimetal under high H

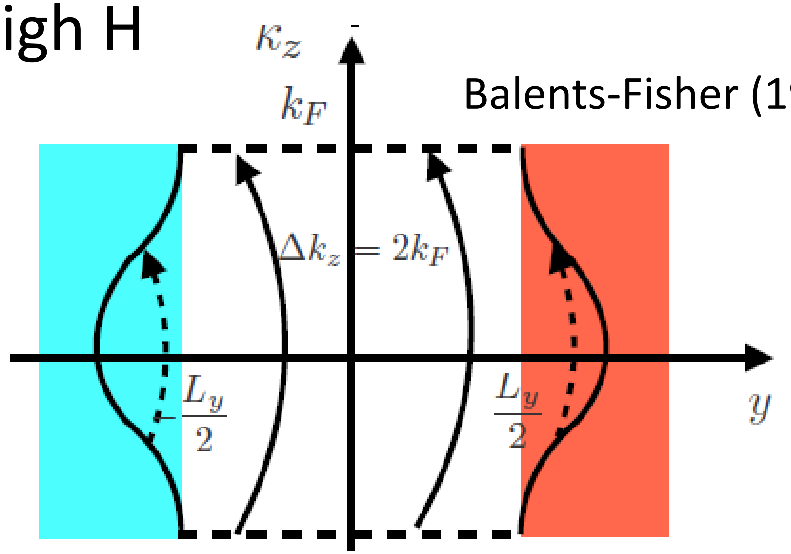

"3D layered Chern band insulator"

◆ RPA Density correlation function

Yoshioka-Fukuyama (1980)

$$\chi_{\mathrm{RPA}}(q_z) = \frac{\chi_0(q_z)}{1 + g\chi_0(q_z)}$$

($g < 0$ **By Fock term)**

$$\chi_0(q_z) = \int \frac{dk_z}{2\pi} \frac{f(k_z) - f(k_z + q_z)}{\varepsilon(k_z) - \varepsilon(k_z + q_z)}$$

$$= \rho(\varepsilon_F) \ln \left| \frac{q + 2k_F}{q - 2k_F} \right|$$

$$\rightarrow \rho(\varepsilon_F) \ln \frac{\Lambda}{k_B T}$$

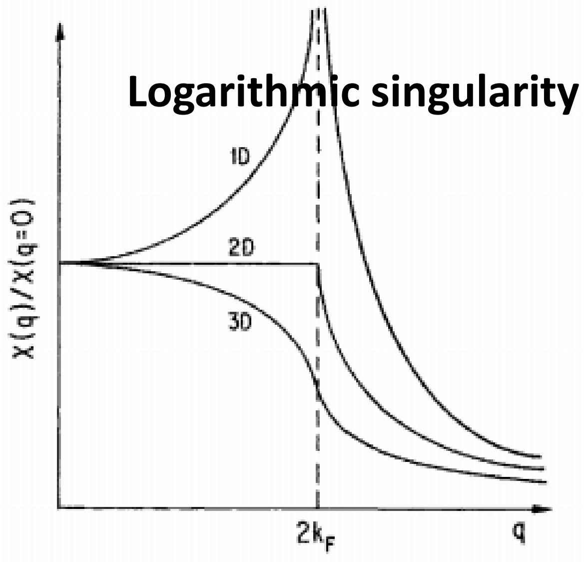

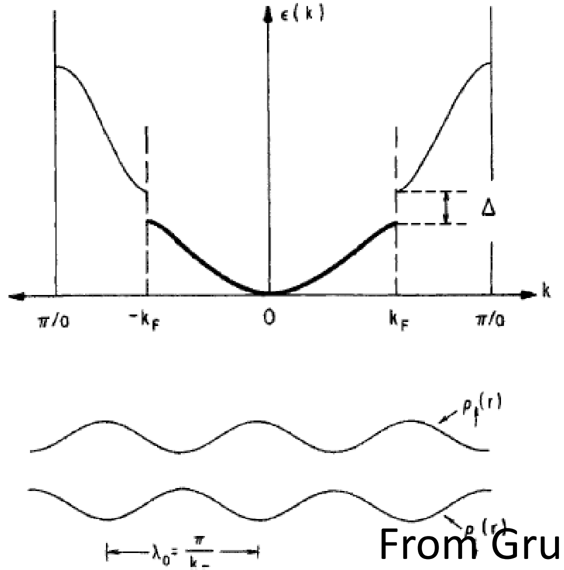

From Gruner

◆ T_c increases on increasing the field H.

$$1 - |g|\rho(\varepsilon_F) \ln \frac{\Lambda}{k_B T_c} = 0$$

$$k_B T_c = \Lambda \exp\left[-\frac{1}{|g|\rho(\varepsilon_F)}\right] = \Lambda \exp\left[-\frac{2\pi\hbar}{|g|SBe}\right]$$

Density Wave (DW) phases which break the translational symmetry along the field direction.

☐ Effect of Disorders on the Density Wave Phase

◆ Effective Boson model for the density wave phases:

Zhang and RS (2017)

Coupled chain model, each 1D chain has two boson fields: $\Pi_j(z)$ *and* $\phi_j(z)$

$$Z = \sum_{\{\sigma_j^z\}} \int D\phi\, D\Pi \,\exp\Big[-\int_0^{\beta} d\tau \int dz \sum_j \Big\{ -i\,\Pi_j(z)\partial_\tau \phi_j(\tau) + \frac{uK\pi}{2}[\Pi_j(z)]^2 + \frac{u}{2\pi K}[\partial_z \phi_j(z)]^2$$
$$\boxed{-\sum_{m\neq j} J_{j-m}\sigma_j^z\sigma_m^z \cos[2\phi_j(z) - 2\phi_m(z)]} + \boxed{\sum_{m\neq j} U_{j-m}\sigma_j^z\sigma_m^z \cos[2\phi_j(z) + 2\phi_m(z)]} \Big\}\Big].$$

$\Pi_j(z)$: current density field along the field direction

$\phi_j(z)$: Displacement field along the field direction (defined for each chain "*j*")

Phason field exhibits a LRO by the Fock term (positive J)

Two-particle backward Scattering at the 1/2 filling

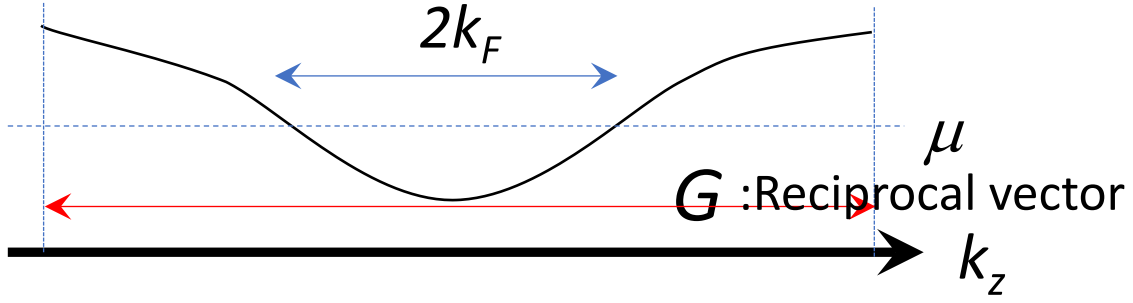

incommensurate filling case: 3D XY model

Commensurate filling case : 3D Zn clock model

$$H^{(1)}_{\rm imp} = \sum_j \int dz\, A_{j,(1)}(z)\{e^{i\lambda_{j,(1)}(z)}\hat{\psi}^{\dagger}_{+,j}(z)\hat{\psi}_{-,j}(z) + \text{H.c.}\},$$: Single-particle backward scattering

➔ $$H^{(1)}_{\rm imp} = \sum_j \int dz A_{j,(1)}(z) \cos\left[2\phi_j(z) + \lambda_{j,(1)}(z)\right]$$: Random "magnetic field" in the XY model

Effect of Disorders on the Density Wave Phase

- Small random "magnetic" field kills the ordered phase in the XY model (DW phase)

Random-Field Instability of the Ordered State of Continuous Symmetry*

Yoseph Imry†
Brookhaven National Laboratory, Upton, New York 11973

and

Shang-keng Ma‡
Department of Physics and Institute for Pure and Applied Physical Sciences, University of California at San Diego, La Jolla, California 92037
(Received 12 August 1975)

We consider phase transitions in systems where the field conjugate to the order parameter is static and random. It is demonstrated that when the order parameter has a continuous symmetry, the ordered state is unstable against an arbitrarily weak random field in less than four dimensions. The borderline dimensionality above which mean-field-theory results hold is six.

Imry-Ma (1975), Sham-Patton (1976), Fukuyama-Lee (1978), . .

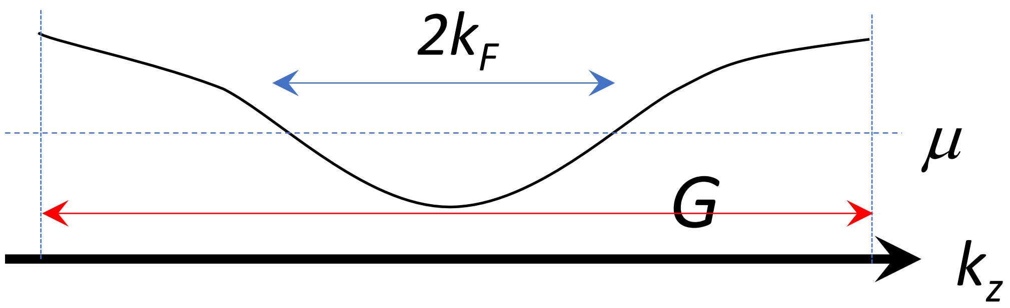

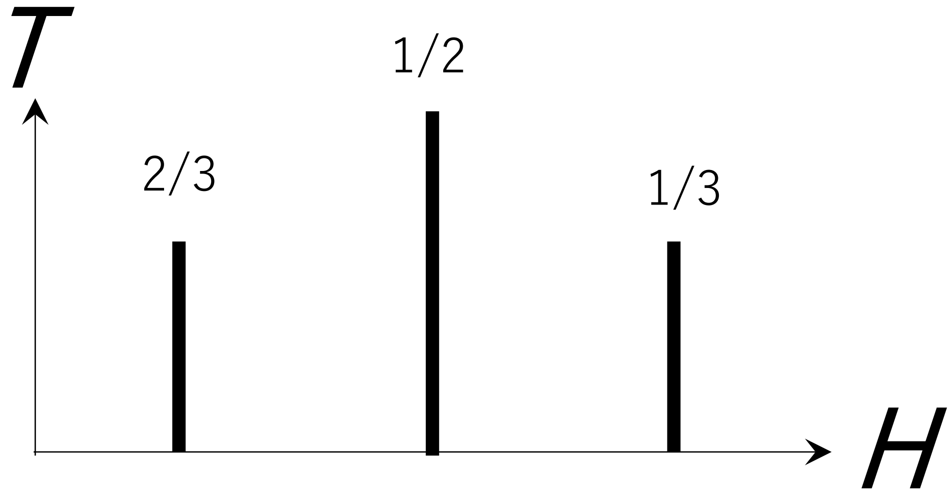

- Incommensurate DW phases which breaks the continuous translational symmetry are unstable against infinitesimally small disorder
- commensurate DW phases which breaks the discrete translational symmetry are not

- **Chemical potential changes as a function of H**

Graphite (3D semimetal) under high H

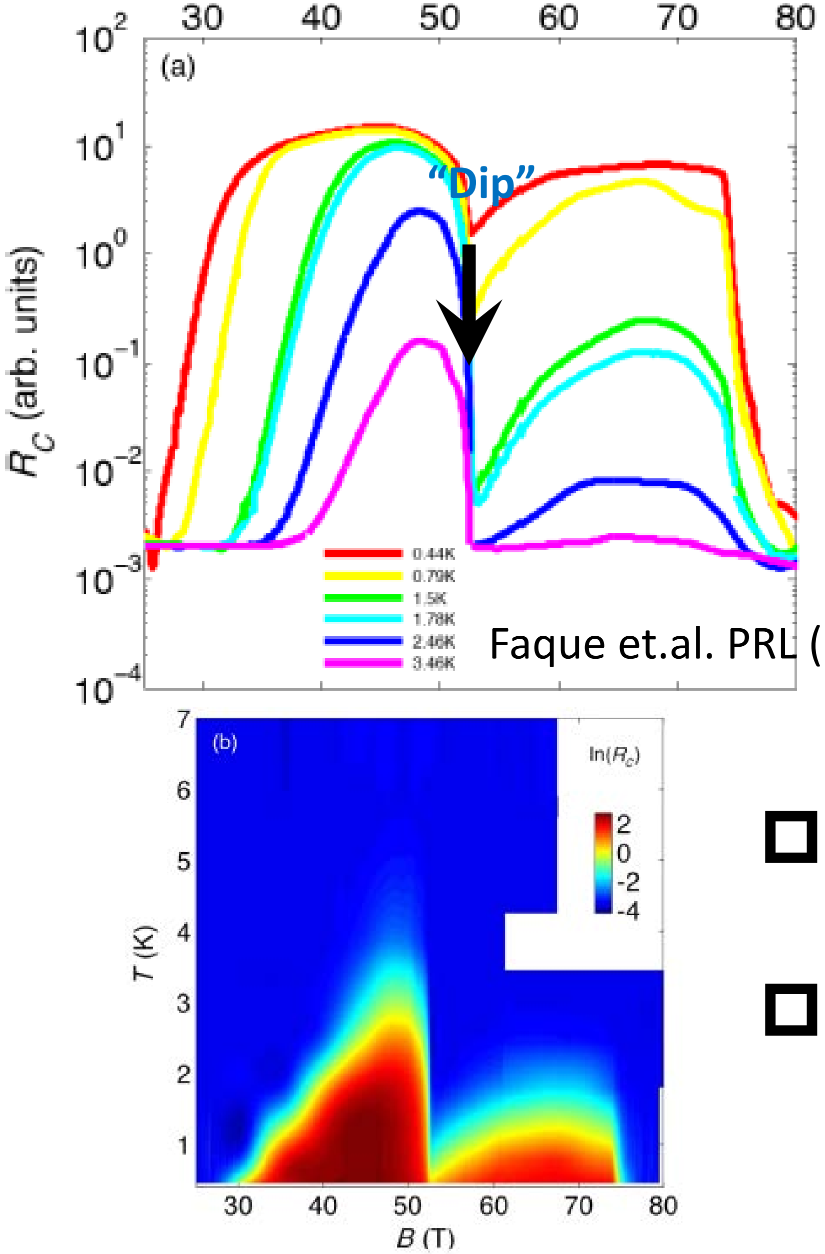

Faque et.al. PRL (2013)

- Graphite is a layered graphene.
- Metal-insulator transition under high field (30T), and insulator-metal transition under 75 T (re-entrant).
- Insulating phase in a *wide* range of field ??

  ←→ Incommensurate DW phases are unstable against infinitesimally small disorder !!

- Re-entrant transition under 75T ??

C.f. $T_c \propto e^{-\frac{1}{|g|B}}$ Yoshioka-Fukuyama (1980)

- Other insulating phase (Neither CDW or SDW phase)

  → **excitonic insulator phase with spin nematic order**

- "Dip" of the resistance reflects **a competition between the insulating phase and com-DW phase.**

Pan and RS, in preparation.

☐ Two-carrier model, Hall conductivity, Charge neutrality region, and Umklapp process

◆ Electron and hole pockets

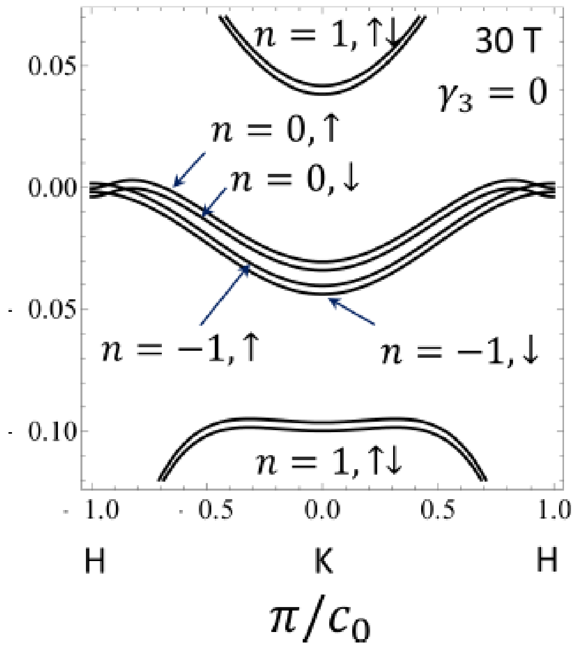

■ According to the band structure calculation, there exist two electron pockets and two hole pockets in 30T<H<50T.

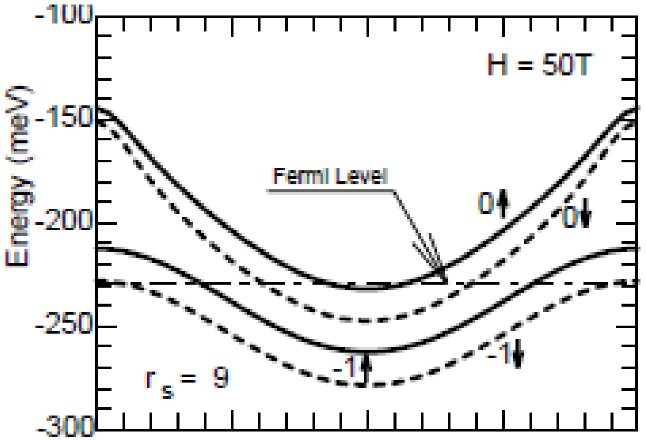

Takada-Goto (1996)

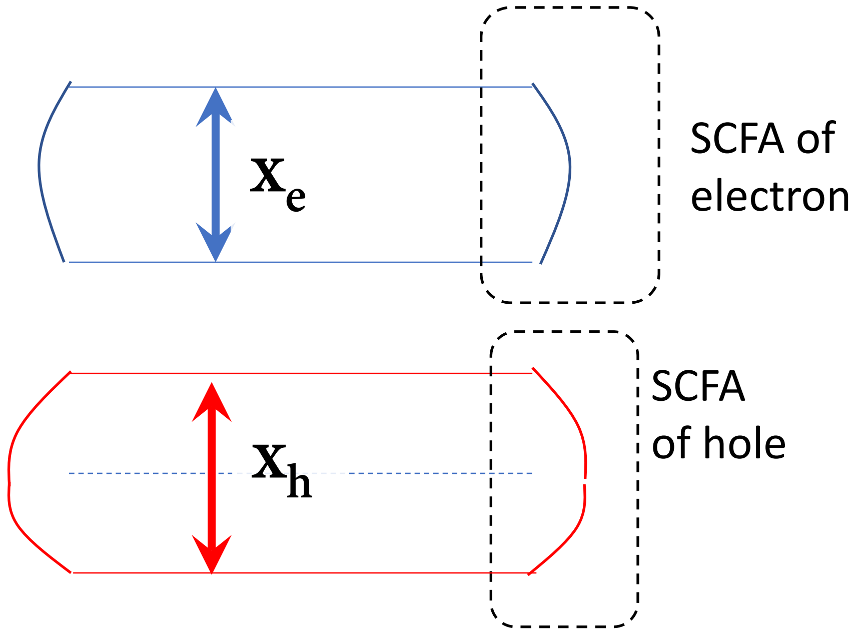

◆ Hall conductivity from the Kubo formula

$$\sigma_{xy}(0) = \frac{(N_e - N_h)ce}{VH}$$

N_e : number of electron carriers
N_h : number of hole carriers

See also Akiba et.al. (2015)

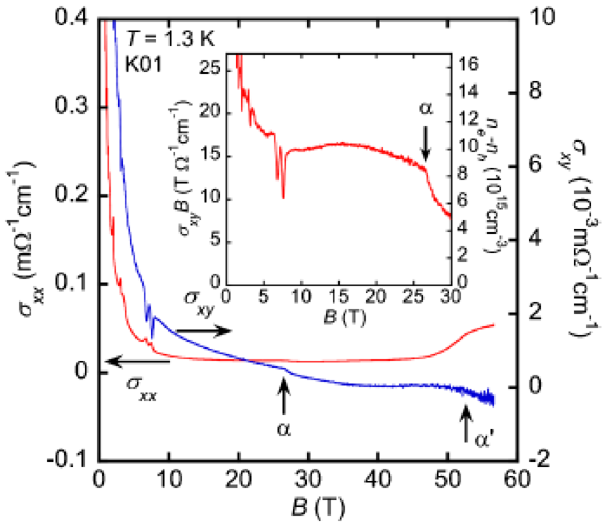

Akiba et.al. JPSJ (2015)

◆ Charge neutrality region (30T<H<57T)

$2\pi/c_0 : x_e - x_h = 1/c_0 : 2\pi l^2 \times (N_e - N_h)$

$= 10^{10} : 2.3 \times 10^6 =$ **$1 : 2.3 \times 10^{-4}$** (H=30T)

➔ **Umklapp scattering process associated with electron and Hole pockets**

◻ excitonic Insulator Phase in graphite under H

Pan and RS, in preparation.

4-bands model (two E-pockets, two H-pockets)

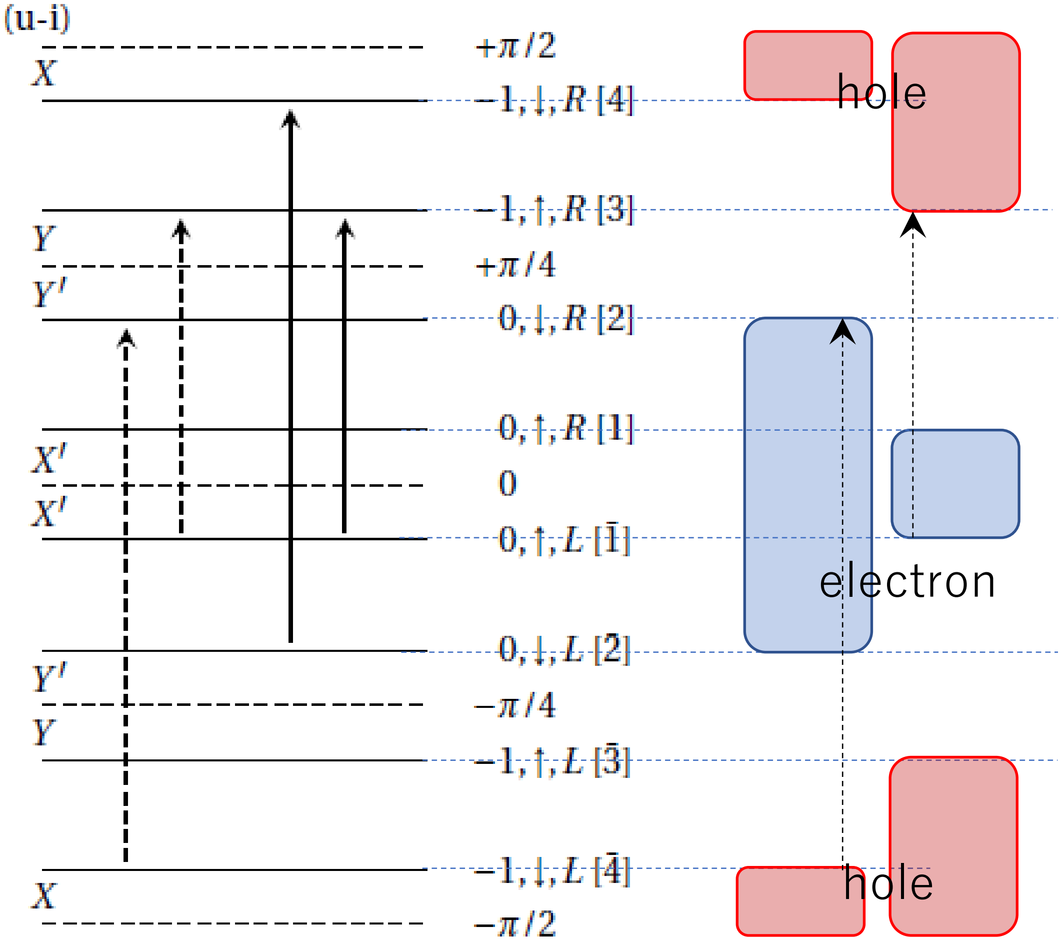

X+Y' = X'+Y

$$1,2,3,4 = (0,\uparrow),(0,\downarrow),(-1,\uparrow),(-1,\downarrow)$$

- Under the charge neutrality condition, there exists eight (or four) different kinds of Umklapp processes, while the following phenomenology does not depend on choice of particular Umklapp process.

$$\int dz\, \psi^\dagger_{R,\uparrow,-1}\psi^\dagger_{R,\downarrow,-1}\psi_{L,\downarrow,0}\psi_{L,\uparrow,0}$$

$$\int dz\, \psi^\dagger_{R,\uparrow,-1}\psi^\dagger_{R,\downarrow,0}\psi_{L,\downarrow,-1}\psi_{L,\uparrow,0}$$

$$H_{\mathrm{umklapp}} = \sum_{j,m,\sigma=\pm} g_{jm}\int dz\cos\Big[(\phi_{3,j}+\phi_{4,j}+\phi_{1,m}+\phi_{2,m})+\sigma(\theta_{3,j}-\theta_{4,j}-\theta_{1,m}+\theta_{2,m})\Big]$$

$(\phi_1+\phi_2+\phi_3+\phi_4)$: Locked 0 or pi ➔ excitonic insulator phase

$(\theta_1-\theta_2-\theta_3+\theta_4)$: Locked 0 or pi ➔ spin nematic order

U(1) spin rotation around the z-axis is broken spontaneously by the ordering of spin quadrupole moment

(But no magnetic dipole moment)

□ excitonic Insulator Phase in graphite under high H

- A tree-level argument on Umklapp term

where K_j : Luttinger parameter for each pocket (j=1,2,3,4)

$$\frac{dg_{jm}}{dl} = \left[2 - \underbrace{\boxed{\frac{1}{4}\sum_{j=1}^{4}\left(K_j + K_j^{-1}\right)\coth\left(\frac{\beta\Lambda}{2}\right)}}_{>2}\right] g_{jm}$$

Pan and RS, in preparation.

Umklapp term is always renormalized to zero near the trivial fixed point in the non-interacting limit.

c.f.

$$H_{\text{umklapp}} = \sum_{j,m,\sigma=\pm} g_{jm} \int dz \cos\left[(\phi_{3,j} + \phi_{4,j} + \phi_{1,m} + \phi_{2,m}) + \sigma(\theta_{3,j} - \theta_{4,j} - \theta_{1,m} + \theta_{2,m})\right]$$

One of the generated terms

- One-loop level RG argument on Umklapp term

Umklapp term generates two new terms which help the umklapp term to grow up in the one-loop level; C>0.

$$\frac{dg_{jm}}{dl} = \left[2 - \frac{1}{4}\sum_{j=1}^{4}\left(K_j + K_j^{-1}\right)\coth\left(\frac{\beta\Lambda}{2}\right)\right] g_{jm} + 2C\sum_l \boxed{g_{jl}\left(h_{lm} + h'_{lm}\right)}$$

$$\frac{dh_{jm}}{dl} = \left[2 - \frac{1}{2}\sum_{j=1}^{2}\left(K_j + K_j^{-1}\right)\coth\left(\frac{\beta\Lambda}{2}\right)\right] h_{jm} + C\sum_l \left(\boxed{g_{jl}g_{lm}} + h_{jl}h_{lm}\right)$$

$$\frac{dh'_{jm}}{dl} = \left[2 - \frac{1}{2}\sum_{j=3}^{4}\left(K_j + K_j^{-1}\right)\coth\left(\frac{\beta\Lambda}{2}\right)\right] h'_{jm} + C\sum_l \left(\boxed{g_{jl}g_{lm}} + h'_{jl}h'_{lm}\right)$$

where $H' = \sum_{j,m,\sigma=\pm} h_{jm} \int dz \cos\left[\Delta_{jm}\left(\phi_1 + \phi_2 + \sigma(-\theta_1 + \theta_2)\right)\right]$

$+ \sum_{j,m,\sigma=\pm} h'_{jm} \int dz \cos\left[\Delta_{jm}\left(\phi_3 + \phi_4 + \sigma(\theta_3 - \theta_4)\right)\right]$

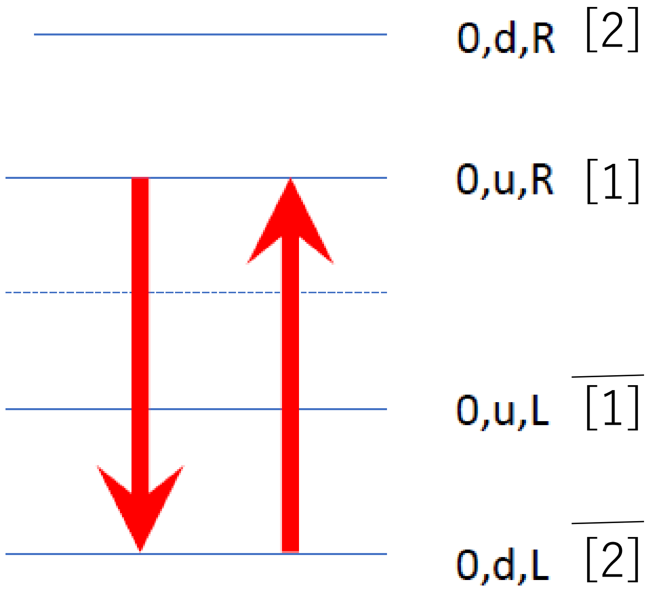

☐ excitonic Insulator Phase in graphite under high H

■ Quantum phase Transition at finite critical interaction strength

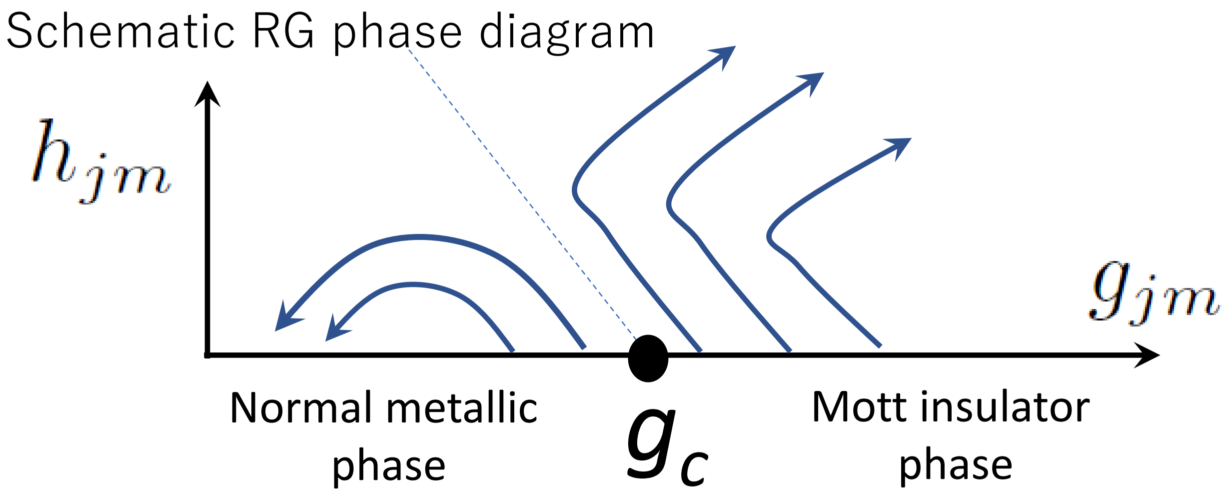

◆ There exists a critical interaction strength "g_c", above which g_{jm} blows up into a larger value, while below which g_{jm} is renormalized to zero.

◆ The critical value increases on increasing T or when the one of the Luttinger parameter "K_j" deviates from 1.

c.f. $$\frac{dg_{jm}}{dl} = \left[2 - \frac{1}{4}\sum_{j=1}^{4}\left(K_j + K_j^{-1}\right)\coth\left(\frac{\beta\Lambda}{2}\right)\right] g_{jm}$$

■ Phenomenology of re-entrant transition in Graphite under high H

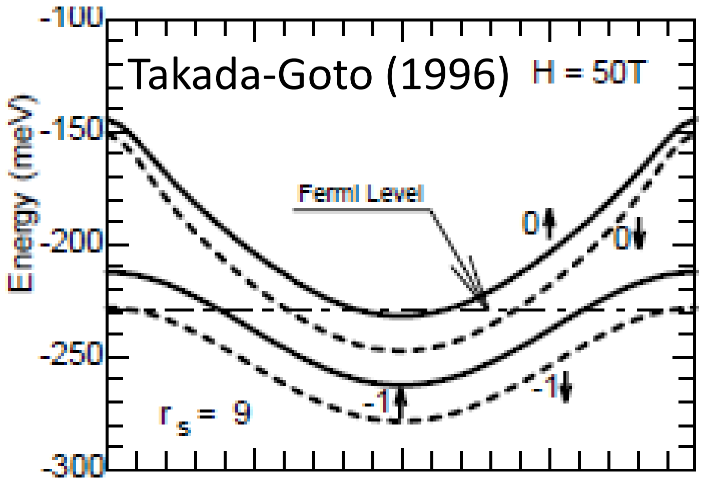

◆ When the outer two branches, (0 up) and (-1,down), are about to "leave" the Fermi level, the Luttinger parameter for these two branches becomes increasingly smaller (velocities smaller).

➔ The critical interaction strength "g_c" becomes larger, which kills the excitonic insulator phase.

◆ In the higher field side of the re-entrant transition, the system still possesses four branches, which lead to a metallic behavior.

□ Summary (Metal-Insulator transition in graphite under high H)

■ Novel interaction-driven MI and IM transition in four bands model

■ The theory gives a natural explanation of phenomenology of Re-entrant MI transition observed in graphite under high H

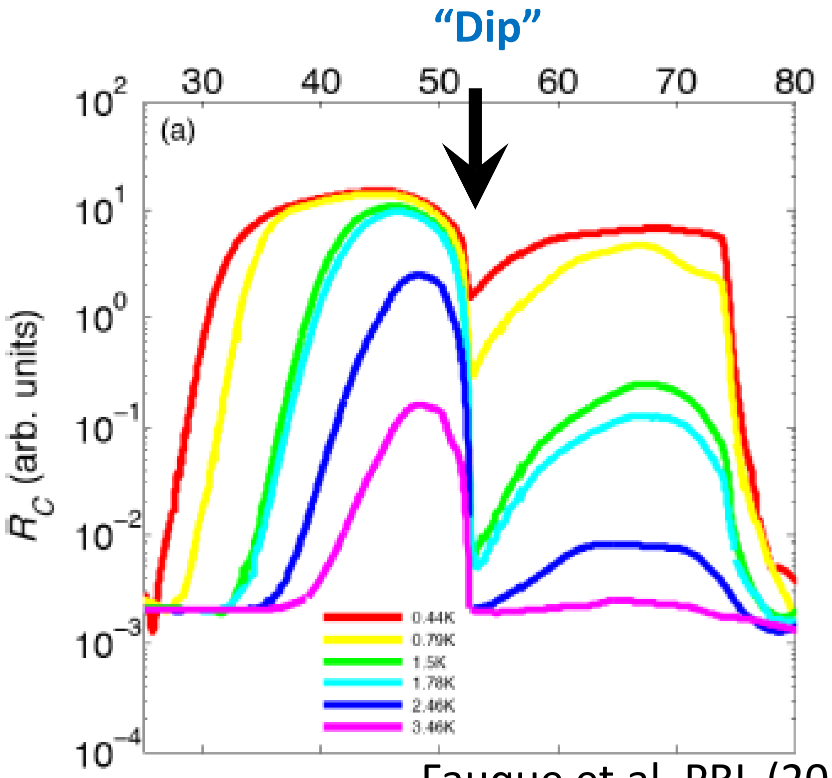

Fauque et.al. PRL (2013)

■ Robust against single-particle backward type disorder, accompanied with spin nematic order

■ Competition between com.-DW and EI ?

■ In-plane metallic behaviour ?

Zhang and RS, Phys. Rev. B 95, 205108 (2017)

Pan and RS, in preparation.

Metal-Insulator Transitions in a model for magnetic Weyl semimetal and graphite under high magnetic field

- Disorder-driven quantum multicriticality in disordered Weyl semimetal

  Luo, Xu, Ohtsuki and RS, ArXiv:1710.00572v2 to appear tomorrow

  Liu, Ohtsuki and RS, Phys. Rev. Lett. 116, 066401 (2016)

  Xunlong Luo (PKU), Shang Liu (PKU -> Harvard),
  Baolong Xu (PKU), Tomi Ohtsuki (Sophia Univ.)

- Correlation-driven metal-insulator transition in graphite under H

  Zhang and RS, Phys. Rev. B 95, 205108 (2017), Pan and RS, in preparation

  Zhiming Pan (PKU), Xiaotian Zhang (PKU), Ryuichi Shindou (PKU)